

Modified magnetohydrodynamics model with wave turbulence: astrophysical applications

E P Kurbatov, A G Zhilkin, D V Bisikalo

DOI: <https://doi.org/10.3367/UFNe.2017.01.038063>

Contents

1. Introduction	798
2. Basic equations	799
2.1 Problem setup; 2.2 Semirelativistic magnetohydrodynamics; 2.3 Taking turbulent perturbations into account	
3. Linearized perturbations	803
3.1 Alfvén waves; 3.2 Double correlators; 3.3 Power spectrum	
4. Sources	807
4.1 Turbulent pressure and stresses; 4.2 Turbulent viscosity; 4.3 Ampère force; 4.4 Turbulent heating	
5. Analysis	811
5.1 Summary of the results; 5.2 Estimates; 5.3 Strong turbulence approximation	
6. Conclusion	814
Appendix. Turbulent sources related to the displacement current	815
A. Equations of motion; B. Entropy equation	
References	816

Abstract. Modeling astrophysical flows in the framework of classical magnetohydrodynamics often encounters significant difficulties due to high (up to relativistic) Alfvén wave velocities. Such situations can arise in modeling the magnetosphere of planets and stars and accretion flows in polars, intermediate polars, and near-neutron stars. In a strongly magnetized plasma, wave turbulence can develop, which can significantly affect the energy balance and the forces determining the plasma dynamics. In this paper, a closed system of equations is obtained for modified magnetohydrodynamics with wave turbulence for a wide range of magnetic fields and turbulence energies. The turbulent flow is described as the sum of the mean flow and perturbations induced by relativistic Alfvén waves. Expressions are derived for the turbulence-induced body force, viscosity, and dissipative heating. An analysis of equations in certain limit cases is performed. It is shown that the proposed approach can be used for modeling a broad class of astrophysical plasma flows.

Keywords: magnetohydrodynamics, turbulence, Alfvén waves, close binary stars

1. Introduction

In many astrophysical problems, the interaction of plasma with the electromagnetic field can be described in the classical magnetohydrodynamics (MHD) approximation for a fully ionized medium (see, e.g., [1]). In this approximation, plasma can be thought of as a conducting fluid in which motions are nonrelativistic. The smallness of the characteristic scales and charge separation times in plasma compared to the scale of the problem enables assuming the electrical neutrality of each elementary plasma volume (see, e.g., [2, 3]). Then, under the quasineutrality condition, the generation of currents in plasma occurs exclusively due to electromagnetic induction.

As a rule, astrophysical flows can be modeled by assuming the ideal MHD approximation, with the magnetic field frozen into matter. This is due to large spatial scales, which in turn lead to large magnetic Reynolds numbers. The finite conductivity of plasma does not play a major role here. Despite the relative simplicity, the MHD approximation allows a quite detailed description of the structure of astrophysical flows. In this way, good agreement with observations can be achieved (see, e.g., [4–9]).

At the same time, we note that criteria underlying the MHD approximation are by no means always met in practice. For example, we consider the plasma flow in polars [10]. These are close binary systems consisting of a red dwarf (donor star) and a white dwarf (accretor star) with a sufficiently strong magnetic field (1–100 MG). The mass exchange causes matter to flow from the envelope of the donor star through the inner Lagrange point L_1 onto the white dwarf. In a typical polar with a component separation of about $2R_\odot$, the magnetic field strength along the accretion stream changes from 10^3 G at the Lagrange point L_1 to 10^7 G

E P Kurbatov, A G Zhilkin, D V Bisikalo Institute of Astronomy,
Russian Academy of Sciences,
ul. Pyatnitskaya 48, 119017 Moscow, Russian Federation
E-mail: kurbatov@inasan.ru, zhilkin@inasan.ru, bisikalo@inasan.ru

Received 15 November 2016, revised 20 January 2017
Uspekhi Fizicheskikh Nauk **187** (8) 857–878 (2017)
DOI: <https://doi.org/10.3367/UFNr.2017.01.038063>
Translated by K A Postnov; edited by A M Semikhatov

near the white dwarf surface. The mass of the white dwarf is about $1M_{\odot}$, which causes an accretion velocity of about 1000 km s^{-1} . The accreting plasma temperature can be estimated to be 10^4 – 10^5 K everywhere outside a close vicinity of the accretion column base, where the temperature is comparable to the kinetic one and reaches 10^8 K [11]. The plasma number density can change along the accretion column from 10^{11} to 10^{15} cm^{-3} [11, 12]. With such parameters, the plasma can be considered fully ionized, quasi-neutral, frozen (the effects of the Ohmic diffusion of the magnetic field are much smaller than the induction effects), and magnetized (the cyclotron radius of electrons is much smaller than the mean free path). By virtue of the last two properties, it is possible to assert that the plasma travels along the magnetic field lines, and thermal pressure effects dominate in the longitudinal direction, while magnetic pressure effects dominate in transverse directions.

Substituting the parameters in the formula for the classical velocity a of Alfvén waves, we find [13]

$$\frac{a}{c} \approx 3 \frac{B}{10^7 \text{ G}} \left(\frac{\rho}{10^{-9} \text{ g cm}^{-3}} \right)^{-1/2}. \quad (1)$$

In other words, on the one hand, velocities of both Alfvén and fast magnetosonic waves in the flow can be relativistic. On the other hand, they significantly exceed both the sound velocity and the plasma bulk velocity. The above estimate of the Alfvén speed already implies that the classical MHD approximation becomes invalid. We note that this situation is not limited to astrophysics. For example, in the auroral zone of Earth's magnetosphere, the Alfvén wave velocity can reach one third of the speed of light [14]. In the polar regions of Jupiter, the Alfvén velocity, calculated according to the classical formula, can exceed the speed of light by a factor of 10 or more. In accretion flows in polars, Alfvén velocity (1) can be several times the speed of light. In white dwarf magnetospheres (in intermediate polars and even more so in polars), the Alfvén velocity can exceed the speed of light by tens, hundreds, and thousands of times. In neutron star magnetospheres, it can be even higher. Quite clearly, under these conditions, the assumptions of classical magnetohydrodynamics become invalid.

The problem under discussion also has a purely technical aspect. Indeed, numerical studies of plasma flows using the classical MHD approximation can encounter substantial difficulties. For example, explicit numerical schemes used in simulations have a limited time step due to the Courant–Friedrichs–Lewy condition (see, e.g., [15]). In a strong magnetic field, this condition can be so strong that further calculations lose practical meaning due to a drastic decrease in the integration step [13, 16]. Some ways to solve this problem have been suggested, for example, in [17–19].

In plasma flows immersed in a strong external magnetic field, in the characteristic dynamical time, Alfvén and magnetosonic waves travel many times in the longitudinal and transverse directions by interacting with themselves and the background flow. In many cases, the interaction of these waves can be considered in the weak (wave) turbulence approximation. This interaction results in the energy redistribution between waves of different scales, leading to a turbulence cascade. This approach was justified in the classical papers on weak turbulence [20, 21]. In particular, this is true for interacting Alfvén waves [22–24] and for magnetosonic waves [25, 26].

Some years ago, we elaborated a semiphenomenological MHD model to describe such astrophysical flows [13, 27, 28]. The model is based on the assumption that the plasma dynamics are fully determined by the slow mean motion established in the background of rapidly propagating MHD waves. To describe such a flow, it is possible to use the averaging over an ensemble of wave pulsations in analogy with the standard approaches used to describe MHD turbulence. In our model, the dynamics of plasma in a strong magnetic field are characterized by a relatively slow motion along magnetic field lines, drifting under the action of external forces (for example, gravity) in the perpendicular direction, as well as by Alfvén and magnetosonic waves propagating with high velocity. In essence, all information about fast pulsations is encoded in the expression for the turbulent viscosity. The values of free parameters were determined from a comparison of numerical solutions obtained in our model with those resulting from rigorous MHD numerical solutions in the case of a weak magnetic field [29]. We successfully applied this method to model the structure of flows in polars and intermediate polars [27, 28, 30–34] (see also monograph [13]).

However, in our previous papers, we derived the model equations from physical considerations by ignoring some important effects, for example, the wave pressure. In this paper, we suggest a more rigorous justification of the model and significantly expand its applicability domain.

2. Basic equations

2.1 Problem setup

MHD waves with a scale smaller than the homogeneity scale of the magnetic field play an important role in MHD. The waves can transport a significant part of the energy of matter, be the source of mechanical stresses, and heat the plasma. In ideal MHD, there are four types of waves: Alfvén, fast and slow magnetosonic, and entropy waves [1]. The Alfvén waves are transverse (incompressible) perturbations in a magnetized plasma, with the phase velocity relative to the medium at rest

$$\frac{\omega}{k} = a \cos \theta \equiv \frac{B}{\sqrt{4\pi\rho}} \cos \theta, \quad (2)$$

where ρ is the matter density, θ is the angle between the wave propagation direction and the homogeneous background magnetic field, and a is the Alfvén velocity.

Fast and slow magnetosonic waves are longitudinal (compressible) perturbations. Their phase velocities are

$$\frac{\omega_{\pm}}{k} = \frac{1}{\sqrt{2}} \left\{ a^2 + c_s^2 \pm [(a^2 + c_s^2)^2 - 4a^2c_s^2 \cos^2 \theta]^{1/2} \right\}^{1/2}, \quad (3)$$

where c_s is the speed of sound. Entropy waves propagate with the velocity of the medium and are related to the entropy transport.

Waves with finite amplitudes can effectively interact. This leads to energy exchange between perturbations of different scales. This can result in the formation of an energy cascade, i.e., an energy flux through the inertial interval extending from the excitation scale to the dissipation scale. Inside the inertial interval of scales, an approximately power-law energy distribution is established [20–26].

Magnetosonic waves are known to decay faster than Alfvén waves. This can be, for example, due to Alfvén waves

running strictly along the background magnetic field, while magnetosonic waves can propagate in all directions. Therefore, the amplitude of magnetosonic perturbations decreases more rapidly with the distance from the source. The compressibility of these waves can lead to radiation losses. The interaction of fast magnetosonic waves, owing to their compressibility, can also lead to substantial energy redistribution into the high-frequency range and to plasma heating, which takes place, for example, in the solar corona [26]. In addition, if the gas-to-magnetic-field pressure ratio is small ($c_s^2/a^2 \ll 1$), the velocity of fast magnetosonic waves becomes comparable to the Alfvén velocity. In this case, fast and slow magnetosonic waves can be ignored, and only Alfvén waves can be taken into account.

A stationary picture of the Alfvén wave turbulence is established via resonance interaction of Alfvén waves that move in opposite directions along magnetic field lines [23, 24, 35, 36]. The amount of energy exchange between the waves depends on their transverse scales. Multiple interactions result in energy redistribution across transverse scales, and an energy cascade arises. Here, the energy distribution over longitudinal scales does not change. The solar wind is an excellent natural laboratory to study Alfvén turbulence (see, e.g., review [37]), in which the turbulence parameters can be directly measured.

The theory of Alfvén turbulence developed in [24] yields the power spectrum in the form

$$E(k_{\parallel}, k_{\perp}) = f(k_{\parallel}) E_{\perp}(k_{\perp}), \quad (4)$$

where $E_{\perp}(k_{\perp}) = E(k_{\parallel} = 0, k_{\perp})$, and the factor $f(k_{\parallel})$ is determined by the conditions at the turbulence region boundary. Thus, Alfvén wave turbulence turns out to be highly anisotropic.

The spectral form of turbulent pulsations can be estimated from simple considerations [36]. We imagine wave turbulence at a transverse scale ℓ as a collection of interacting wave packets with the total energy v_{ℓ}^2 . We let τ denote the interaction time of a pair of wave packets. Over this time interval, the wave energy changes little, by $\delta v_{\ell}^2 \sim (\tau v_{\ell}^2/\ell)^2$, and for a significant change, $N_{\ell} \sim v_{\ell}^2/\delta v_{\ell}^2$ interactions are needed, which means that the characteristic time of energy redistribution is

$$N_{\ell} \tau \sim \frac{\ell^2}{\tau v_{\ell}^2}. \quad (5)$$

We let ϵ denote the energy flux through the energy cascade. In the case of developed turbulence, it does not depend on the pulsation scale and can be expressed as

$$\epsilon \sim \frac{v_{\ell}^2}{N_{\ell} \tau} \sim \tau \frac{v_{\ell}^4}{\ell^2}. \quad (6)$$

This yields the energy distribution of pulsations over scales:

$$v_{\ell}^2 \sim \left(\frac{\epsilon}{\tau}\right)^{1/2} \ell. \quad (7)$$

Expressing the scale in terms of the wavenumber, $k_{\perp} = \ell^{-1}$, and the energy in terms of the energy spectrum, $v_{\ell}^2 \sim k_{\perp} E_{\perp}(k_{\perp})$, yields

$$E_{\perp}(k_{\perp}) \sim \left(\frac{\epsilon}{\tau}\right)^{1/2} k_{\perp}^{-2}. \quad (8)$$

The time of turbulence development can now be estimated as

$$\max_{\ell} (N_{\ell} \tau) \sim \frac{L_{\perp}}{\sqrt{\epsilon \tau}}, \quad (9)$$

where L_{\perp} is the maximum transverse turbulence scale. The time τ must be of the order of the Alfvén time for the longitudinal scale of the problem: $\tau \sim L_{\parallel}/a$.

Turbulence can have a significant effect on the MHD flow by changing both the energy balance and forces acting in the medium. It seems possible to take the Alfvén turbulence effects into account in the MHD approximation. To do this, we suggest considering a turbulent flow as the sum of the ‘mean’ flow and perturbations. Averaging over an ensemble of perturbations leads to the appearance of additional terms in the equations, due to perturbation correlations. By specifying the statistical properties of perturbations, it is possible to obtain a closed system of equations. Such an approach has been used in many studies, both in hydrodynamics and MHD (see, e.g., [38, 39]). One of the distinctive features of the present study is that the perturbation is treated as an ensemble of Alfvén waves whose statistics correspond to the developed Alfvén turbulence [24].

We mentioned above that in some applications, the velocity of Alfvén waves can reach relativistic and super-relativistic values, while the mean flow remains nonrelativistic. It turns out that the presence of electromagnetic phenomena with relativistic spatial and temporal scalings causes the appearance of additional terms in the MHD equations. As we see in what follows, accounting for the displacement current in the presence of Alfvén turbulence gives rise to an additional force acting on the plasma.

2.2 Semirelativistic magnetohydrodynamics

We define all thermodynamic quantities in the local reference frame comoving with the flow and the components of vectors and tensors in the inertial ‘laboratory’ frame. The joint equations of the relativistic flow dynamics and electromagnetic field in this frame are [13, 40]

$$\frac{\partial}{\partial t}(\Gamma \rho) + \nabla(\Gamma \rho \mathbf{v}) = 0, \quad (10)$$

$$\frac{\partial}{\partial t} \left[\frac{\Gamma^2}{c^2} (e + P) \mathbf{v} + \frac{\mathbf{S}}{c^2} \right] + \nabla \left[\frac{\Gamma^2}{c^2} (e + P) \mathbf{v} \otimes \mathbf{v} + P \hat{\mathbf{I}} + \hat{\mathbf{\Pi}} \right] = 0, \quad (11)$$

$$\frac{\partial}{\partial t} [\Gamma^2 (e + P) - P - \Gamma \rho c^2 + w] + \nabla \left\{ [\Gamma^2 (e + P) - \Gamma \rho c^2] \mathbf{v} + \mathbf{S} \right\} = 0. \quad (12)$$

Here, ρ is the volume mass density, \mathbf{v} is the mass velocity, P is the pressure, e is the volume energy density, including the rest-mass energy,

$$e = \rho c^2 + \rho \epsilon, \quad (13)$$

ϵ is the thermal energy density per particle, and $\hat{\mathbf{I}}$ is the three-dimensional unit tensor. The Lorentz factor is

$$\Gamma = \left(1 - \frac{v^2}{c^2}\right)^{-1/2}, \quad (14)$$

the Poynting energy flux vector is

$$\mathbf{S} = \frac{c}{4\pi} \mathbf{E} \times \mathbf{B}, \quad (15)$$

the volume density of the electromagnetic energy is

$$w = \frac{E^2 + B^2}{8\pi}, \quad (16)$$

and the Maxwell stress tensor is

$$\hat{\mathbf{P}} = w\hat{\mathbf{I}} - \frac{\mathbf{E} \otimes \mathbf{E} + \mathbf{B} \otimes \mathbf{B}}{4\pi}, \quad (17)$$

where \mathbf{E} and \mathbf{B} are the electric and magnetic field strength vectors. The symbol \otimes denotes the tensor product, i.e., for example, $\mathbf{E} \otimes \mathbf{B}$ yields $E_i B_k$. We assume the sound velocity in the medium to be much less than the speed of light and assume the perfect-gas equation of state with the adiabatic exponent γ such that

$$P = (\gamma - 1)\rho\varepsilon. \quad (18)$$

It can be shown that up to a temperature of 10^9 K, relativistic corrections to this relation are insignificant. In general, the equation of state is more complex [14].

We assume the medium velocity to be much less than the speed of light; then $\Gamma \approx 1$, $e \approx \rho\varepsilon$, and Eqns (10)–(12) reduce to

$$\frac{\partial \rho}{\partial t} + \nabla(\rho\mathbf{v}) = 0, \quad (19)$$

$$\frac{\partial}{\partial t} \left(\rho\mathbf{v} + \frac{\mathbf{S}}{c^2} \right) + \nabla \left(\rho\mathbf{v} \otimes \mathbf{v} + P\hat{\mathbf{I}} + \hat{\mathbf{P}} \right) = 0, \quad (20)$$

$$\frac{\partial}{\partial t} \left(\rho\varepsilon + \rho \frac{v^2}{2} + w \right) + \nabla \left[\left(\rho\varepsilon + \rho \frac{v^2}{2} + P \right) \mathbf{v} + \mathbf{S} \right] = 0. \quad (21)$$

System of equations (19)–(21) should be complemented with the Maxwell equations

$$\text{rot } \mathbf{E} = -\frac{1}{c} \frac{\partial \mathbf{B}}{\partial t}, \quad (22)$$

$$\nabla \mathbf{E} = 4\pi q, \quad (23)$$

$$\text{rot } \mathbf{B} = \frac{4\pi}{c} \mathbf{j} + \frac{1}{c} \frac{\partial \mathbf{E}}{\partial t}, \quad (24)$$

$$\nabla \mathbf{B} = 0, \quad (25)$$

where q is the volume charge density in the comoving frame and \mathbf{j} is the conductivity current density.

With the given charge density q and current density \mathbf{j} , Eqns (18)–(21) jointly with Maxwell equations (22)–(25) form a complete system of equations. The current density is to be determined from Ohm's law with a finite conductivity σ ,

$$\mathbf{j} = q\mathbf{v} + \sigma \left(\mathbf{E} + \frac{\mathbf{v}}{c} \times \mathbf{B} \right). \quad (26)$$

The first term in the right-hand side of (26) is the convection current. It is due to the presence of noncompensated electric charges in the plasma with a charge density q . The second term describes the conductivity current.

We estimate different effects on the plasma flow and field generation. From Eqns (24) and Ohm's law (26), we can derive the magnetic field induction equation

$$\frac{\partial \mathbf{B}}{\partial t} - \text{rot} \left(\mathbf{v} \times \mathbf{B} - \frac{c^2}{4\pi\sigma} \text{rot } \mathbf{B} + \frac{c}{4\pi\sigma} \frac{\partial \mathbf{E}}{\partial t} + \frac{c}{\sigma} q\mathbf{v} \right) = 0. \quad (27)$$

The last two terms in the left-hand side are respectively responsible for the magnetic field generation due to the displacement current and the convective current. The displacement current is due to electromagnetic waves. The appearance of the convective current in a quasineutral plasma is due to the charge separation of electrons and ions. The noncompensated electric charge and the displacement current appear on short time scales and small spatial variability scales in plasma.

The electric field induction is described by Eqn (24) and Ohm's law (26):

$$\frac{1}{4\pi} \frac{\partial \mathbf{E}}{\partial t} + q\mathbf{v} + \sigma \left(\mathbf{E} + \frac{\mathbf{v}}{c} \times \mathbf{B} \right) - \frac{c}{4\pi} \text{rot } \mathbf{B} = 0. \quad (28)$$

The divergence of this equation yields the charge induction law:

$$\frac{\partial q}{\partial t} + \nabla \mathbf{j} = 0 \quad (29)$$

or

$$\frac{\partial q}{\partial t} + \nabla(q\mathbf{v}) = -\nabla \left(\sigma \mathbf{E} + \sigma \frac{\mathbf{v}}{c} \times \mathbf{B} \right). \quad (30)$$

The directed charge generation is due to the second term in the right-hand side of this equation, while the first term provides its dissipation. Let L and T be the characteristic spatial scale and the time variability scale of the problem:

$$\nabla \sim \frac{1}{L}, \quad \frac{\partial}{\partial t} \sim \frac{1}{T}. \quad (31)$$

Using Eqn (23), it is possible to estimate the charge density in the stationary limit of Eqn (30) as

$$|q| \sim \frac{v}{cL} B, \quad (32)$$

and using Eqn (22), we can estimate the electric field strength:

$$|\mathbf{E}| \sim \frac{L}{cT} B. \quad (33)$$

The terms in Eqn (27) compare as the ratio

$$1 : \frac{vT}{L} : \frac{c^2 T}{\sigma L^2} : \frac{1}{\sigma T} : \frac{v^2 T}{\sigma L^2}. \quad (34)$$

We assume that the scale ratio L/T is of the order of the plasma velocity v ; the above ratios can then be rewritten as

$$1 : 1 : \frac{1}{\sigma T} \frac{c^2}{v^2} : \frac{1}{\sigma T} : \frac{1}{\sigma T}. \quad (35)$$

The conductivity σ is usually high in astrophysical problems, and hence $\sigma T \gg 1$. Clearly, in this case the displacement current and the conductivity current are of the same order of smallness and are much smaller than other terms, the induction term ($\text{rot}(\mathbf{v} \times \mathbf{B})$) and the dissipative term ($\propto \nabla^2 \mathbf{B}$). Hence, magnetic field induction equation (27) takes the form

$$\frac{\partial \mathbf{B}}{\partial t} - \text{rot} \left(\mathbf{v} \times \mathbf{B} + \frac{c^2}{4\pi\sigma} \text{rot } \mathbf{B} \right) = 0. \quad (36)$$

If there are electromagnetic perturbations in the system with short time variability scales (for example, electromagnetic waves, for which $L/T \sim c$), the terms in (27) compare as

$$1 : \frac{v}{c} : \frac{1}{\sigma T} : \frac{1}{\sigma T} : \frac{1}{\sigma T} \frac{v^2}{c^2}. \quad (37)$$

Because $\sigma T \gg q$, only the inductive term remains to be a source of the magnetic field:

$$\frac{\partial \mathbf{B}}{\partial t} - \text{rot}(\mathbf{v} \times \mathbf{B}) = 0. \quad (38)$$

Thus, in the approximation $\sigma T \gg 1$, the contributions from the displacement current and electric charge to the magnetic field induction equation can be ignored both in the case of slow motion, $L/T \sim v \ll c$, and for electromagnetic perturbations, $L/T \sim c$.

A similar analysis of the electric field induction equation in the case $L/T \sim v$ yields the relation

$$\mathbf{E} + \frac{\mathbf{v}}{c} \times \mathbf{B} = \frac{c}{4\pi\sigma} \text{rot} \mathbf{B}. \quad (39)$$

If $\sigma T \gg 1$, the right-hand side of this expression can be ignored. The resulting relation

$$\mathbf{E} = -\frac{\mathbf{v}}{c} \times \mathbf{B} \quad (40)$$

can be used as an approximation for the electric field strength instead of induction equation (28). We note that in the case of small-scale perturbations ($L/T \sim c$), the last equation together with Maxwell equation (22) is equivalent to Eqn (38).

To proceed, it is convenient to transform equation of motion (20) and energy equation (21). It follows from the Maxwell equations that

$$\frac{1}{c^2} \frac{\partial \mathbf{S}}{\partial t} + \nabla \hat{\Pi} = -q\mathbf{E} - \frac{1}{c} \mathbf{j} \times \mathbf{B}, \quad (41)$$

and therefore Eqn (20) can be rewritten as

$$\frac{\partial \mathbf{v}}{\partial t} + (\mathbf{v}\nabla)\mathbf{v} = -\frac{\nabla P}{\rho} - \frac{\mathbf{B} \times \text{rot} \mathbf{B}}{4\pi\rho} + \frac{q\mathbf{E}}{\rho} - \frac{1}{4\pi\rho c} \frac{\partial \mathbf{E}}{\partial t} \times \mathbf{B}. \quad (42)$$

Here, we used continuity equation (19) and expressed the current from Maxwell equation (24).

Energy conservation law (21) can be changed by the equation for entropy. Ignoring flows with discontinuities and other dissipation effects (for example, diffusion and viscosity), we are left with only one source of entropy—Ohm's conductivity. In the relativistic form, the entropy equation becomes [41]

$$\frac{\partial}{\partial t}(\Gamma\rho s) + \nabla(\Gamma\rho s\mathbf{v}) - \frac{\mathbf{j}^2}{\sigma T} = 0. \quad (43)$$

Here, s is the entropy per unit mass, which is related to the pressure and density by the equation

$$P = \frac{k_B}{m} \rho T = \left(\frac{\rho}{m}\right)^\gamma \exp\left[(\gamma-1)\frac{m}{k_B}s\right], \quad (44)$$

where T is the temperature, m is the mass of gas particles, and k_B is the Boltzmann constant. For nonrelativistic flows,

$$\frac{\partial s}{\partial t} + (\mathbf{v}\nabla)s = \frac{c^2}{(4\pi)^2\sigma\rho T} \left(|\text{rot} \mathbf{B}|^2 - \frac{1}{c} \frac{\partial \mathbf{E}}{\partial t} \text{rot} \mathbf{B} + \frac{1}{c^2} \left| \frac{\partial \mathbf{E}}{\partial t} \right|^2 \right). \quad (45)$$

It is easy to show that the effect of the displacement current on the flow motion is noticeable only for relativistic perturbations ($L/T \sim c$):

$$|\mathbf{B} \times \text{rot} \mathbf{B}| : \left| \frac{1}{c} \frac{\partial \mathbf{E}}{\partial t} \times \mathbf{B} \right| \sim c^2 : \frac{L^2}{T^2}. \quad (46)$$

The same holds for the displacement current effect in entropy equation (45).

For the induced charge effects to be important, relativistic perturbations alone are insufficient. It is necessary that the plasma bulk velocity also be relativistic:

$$|\mathbf{B} \times \text{rot} \mathbf{B}| : |q\mathbf{E}| \sim c^2 : \frac{L}{T} v. \quad (47)$$

This case is beyond the scope of the semirelativistic model; therefore, we disregard the volume charge density effects in what follows.

2.3 Taking turbulent perturbations into account

We assume that we can separate an MHD flow into slow and fast parts. For the slow part, spatial and temporal scales have the nonrelativistic ratio L/T , and we can therefore ignore the displacement current and volume charge density. The fast part corresponds to short-period perturbations. If perturbations have sufficiently small variability scales and high velocities, taking their influence on the slow flow into account requires relativistic effects—the electric charge induction and displacement current.

The perturbation field is to be defined by statistical properties of the developed Alfvén wave turbulence. The turbulence elements include Alfvén waves (incompressible transverse perturbations propagating along the background magnetic field in plasma). In general, they include perturbations of the velocity, electric and magnetic fields, and charges.

We represent all quantities in the equations as the sum of ‘slow’ and ‘fast’ terms, with the latter regarded as perturbations:

$$\mathbf{v} \mapsto \mathbf{v} + \delta\mathbf{v}, \quad \mathbf{B} \mapsto \mathbf{B} + \delta\mathbf{B}, \quad \mathbf{E} \mapsto \mathbf{E} + \delta\mathbf{E}. \quad (48)$$

In Section 2.2, we showed that estimate (40) for the electric field strength is also valid when fast waves are present in the plasma. Therefore, the electric field perturbations can be determined from the expression

$$\delta\mathbf{E} = -\frac{\delta\mathbf{v}}{c} \times \mathbf{B} - \frac{\mathbf{v}}{c} \times \delta\mathbf{B} - \frac{\delta\mathbf{v}}{c} \times \delta\mathbf{B}. \quad (49)$$

Substituting definitions (48) and (49) in continuity equation (19), magnetic induction equation (27), Euler equation (20), and entropy equation (45) results in the appearance of additional terms containing linear, quadratic, and cubic perturbations. By specifying the collection of perturbations as a statistical ensemble, we can average the equations over perturbations. Setting the mean values of perturbations to zero and disregarding third-order terms, we eventually obtain evolutionary equations for ‘slow’ variables.

They contain sources that are defined in terms of pair correlators of the ‘fast’ variables.

Alfvén perturbations are incompressible, and therefore continuity equation (19) does not change. The Euler equation after averaging takes the form

$$\begin{aligned} \frac{\partial \mathbf{v}}{\partial t} + (\mathbf{v}\nabla)\mathbf{v} + \frac{\nabla P}{\rho} + \frac{\mathbf{B} \times \text{rot } \mathbf{B}}{4\pi\rho} \\ = -\nabla\langle\delta\mathbf{v} \otimes \delta\mathbf{v}\rangle + \frac{\nabla\langle\delta\mathbf{B} \otimes \delta\mathbf{B}\rangle}{4\pi\rho} - \frac{\nabla\langle|\delta\mathbf{B}|^2\rangle}{8\pi\rho} \\ - \frac{1}{4\pi\rho}\left\langle\frac{1}{c}\frac{\partial\delta^{(1)}\mathbf{E}}{\partial t} \times \delta\mathbf{B}\right\rangle - \frac{1}{4\pi\rho}\left\langle\frac{1}{c}\frac{\partial\delta^{(2)}\mathbf{E}}{\partial t} \times \mathbf{B}\right\rangle, \end{aligned} \quad (50)$$

where $\delta^{(1)}\mathbf{E}$ and $\delta^{(2)}\mathbf{E}$ are the linear and quadratic parts of electric field perturbations (49). The induction equation after averaging takes the form

$$\frac{\partial \mathbf{B}}{\partial t} - \text{rot}(\mathbf{v} \times \mathbf{B} - \eta \text{rot } \mathbf{B}) = \text{rot}(\delta\mathbf{v} \times \delta\mathbf{B}). \quad (51)$$

We here let $\eta = c^2/(4\pi\sigma)$ denote the Ohmic magnetic viscosity coefficient. The entropy equation becomes

$$\begin{aligned} \frac{\partial s}{\partial t} + \nabla\langle s\mathbf{v}\rangle - \frac{\eta}{T}\frac{|\text{rot } \mathbf{B}|^2}{4\pi\rho} = \frac{\eta}{T}\frac{|\text{rot } \delta\mathbf{B}|^2}{4\pi\rho} \\ - \frac{2\eta}{T}\frac{1}{4\pi\rho}\left\langle\frac{1}{c}\frac{\partial\delta^{(1)}\mathbf{E}}{\partial t} \text{rot } \delta\mathbf{B}\right\rangle - \frac{2\eta}{T}\frac{1}{4\pi\rho}\left\langle\frac{1}{c}\frac{\partial\delta^{(2)}\mathbf{E}}{\partial t} \text{rot } \mathbf{B}\right\rangle \\ + \frac{\eta}{T}\frac{1}{4\pi\rho}\left\langle\left|\frac{1}{c}\frac{\partial\delta^{(1)}\mathbf{E}}{\partial t}\right|^2\right\rangle + \frac{2\eta}{T}\frac{1}{4\pi\rho}\left\langle\frac{1}{c^2}\frac{\partial\delta^{(2)}\mathbf{E}}{\partial t} \frac{\partial\mathbf{E}}{\partial t}\right\rangle. \end{aligned} \quad (52)$$

Turbulent sources in the right-hand sides of (50)–(52) should be expressed from the solution of equations for perturbations. These equations can contain higher-order perturbations. Thus, a chain of equations (generally speaking, infinite) for correlators of various orders arises. In [38], this method was used to take the effects of compressible hydrodynamic turbulence on the background of slow motion into account, and turbulent sources were calculated up to the fourth order. In [39], an ensemble of small-scale perturbations was introduced to subgrid the modeling of compressible MHD turbulence. To complete the equations, the authors of that paper used model expressions for mechanical and magnetic stress tensors induced by turbulence.

In this paper, to compute turbulent sources in Eqns (50)–(52), we rely on the results in [24], where the power spectrum of Alfvén wave turbulence was obtained. In that paper, the Alfvén wave turbulence was represented as an ensemble of spatial Fourier harmonics each of which corresponds to a separate Alfvén wave. We adopt the same approach. Here, the pair correlators that correspond to turbulent sources are expressed through the power spectrum of the ensemble of Alfvén perturbations. The accuracy of this approach turns out to be insufficient, for example, to compute turbulent viscosity effects (see Section 4). In such cases, the pair correlators are calculated in the τ -relaxation approximation using the spectrum from [24] as the zeroth approximation.

3. Linearized perturbations

To calculate turbulent sources in Eqns (50)–(52), we need expressions for Alfvén wave amplitudes, as well as more general expressions for amplitudes of small perturbations

propagating in a weakly inhomogeneous background flow. We write the linearized equation for perturbations (48) by ignoring the displacement current effects in the background flow:

$$\begin{aligned} \frac{\partial\delta\mathbf{v}}{\partial t} + (\mathbf{v}\nabla)\delta\mathbf{v} + (\delta\mathbf{v}\nabla)\mathbf{v} + \frac{\delta\mathbf{B} \times \text{rot } \mathbf{B}}{4\pi\rho} \\ + \frac{(\nabla \otimes \delta\mathbf{B})\mathbf{B} - (\mathbf{B}\nabla)\delta\mathbf{B}}{4\pi\rho} + \frac{1}{4\pi\rho c}\frac{\partial\delta^{(1)}\mathbf{E}}{\partial t} \times \mathbf{B} = 0, \end{aligned} \quad (53)$$

$$\begin{aligned} \frac{\partial\delta\mathbf{B}}{\partial t} + (\mathbf{v}\nabla)\delta\mathbf{B} - (\mathbf{B}\nabla)\delta\mathbf{v} + (\delta\mathbf{v}\nabla)\mathbf{B} - (\delta\mathbf{B}\nabla)\mathbf{v} + (\nabla\mathbf{v})\delta\mathbf{B} \\ + \mathbf{B}(\nabla\delta\mathbf{v}) + \text{rot}(\eta \text{rot } \delta\mathbf{B}) = 0. \end{aligned} \quad (54)$$

Here, the electric field perturbations include only linear components of Eqn (49).

3.1 Alfvén waves

In view of the properties of Alfvén turbulence, we are interested only in incompressible velocity and magnetic field perturbations whose amplitude vectors are transverse to the background field. We assume that the background density, velocity, and magnetic field change little on the characteristic variability scale of perturbations, and therefore their derivative can be ignored. For convenience, we express the magnetic field vectors in velocity units:

$$\mathbf{a} = \frac{\mathbf{B}}{\sqrt{4\pi\rho}}, \quad \delta\mathbf{b} = \frac{\delta\mathbf{B}}{\sqrt{4\pi\rho}}. \quad (55)$$

We define the Fourier transformation of a perturbation $\delta f(t, \mathbf{x})$:

$$\delta\tilde{f}_{\omega, \mathbf{k}} = \frac{1}{(2\pi)^4} \int dt d^3x \exp(i\omega t - i\mathbf{k}\mathbf{x}) \delta f(t, \mathbf{x}), \quad (56)$$

$$\delta f(t, \mathbf{x}) = \int d\omega d^3k \exp(-i\omega t + i\mathbf{k}\mathbf{x}) \delta\tilde{f}_{\omega, \mathbf{k}}. \quad (57)$$

Below in this section, we omit the indices of Fourier amplitudes.

In the harmonic representation, linearized Euler equation (53) and induction equation (54) with account for (49) and (55) take the form

$$(\omega - \mathbf{v}\mathbf{k})\delta\tilde{\mathbf{v}} + (\mathbf{a}\mathbf{k})\delta\tilde{\mathbf{b}} + \frac{a^2}{c^2}\omega\delta\tilde{\mathbf{v}} - \frac{(\mathbf{a}\mathbf{v})}{c^2}\omega\delta\tilde{\mathbf{b}} = 0, \quad (58)$$

$$(\mathbf{a}\mathbf{k})\delta\tilde{\mathbf{v}} + (\omega - \mathbf{v}\mathbf{k})\delta\tilde{\mathbf{b}} = 0. \quad (59)$$

Here, we neglect the magnetic viscosity η and take into account that the waves are incompressible and have a polarization orthogonal to the background magnetic field:

$$\mathbf{k}\delta\tilde{\mathbf{v}} = \mathbf{k}\delta\tilde{\mathbf{b}} = 0, \quad (60)$$

$$\mathbf{a}\delta\tilde{\mathbf{v}} = \mathbf{a}\delta\tilde{\mathbf{b}} = 0. \quad (61)$$

We define the mutually orthogonal unit vectors \mathbf{e}_{\parallel} , \mathbf{e}_{\perp} , and \mathbf{e}_n as follows:

$$\mathbf{a} = \mathbf{e}_{\parallel}a, \quad \mathbf{k} = \mathbf{e}_{\parallel}k_{\parallel} + \mathbf{e}_{\perp}k_{\perp}, \quad \mathbf{e}_n = \mathbf{e}_{\parallel} \times \mathbf{e}_{\perp}. \quad (62)$$

Alfvén wave properties (60) and (61) imply that their amplitude vectors are orthogonal to the vectors \mathbf{a} and \mathbf{k} simultaneously:

$$\delta\tilde{\mathbf{v}} = \mathbf{e}_n\delta\tilde{v}, \quad \delta\tilde{\mathbf{b}} = \mathbf{e}_n\delta\tilde{b}. \quad (63)$$

Assuming that $\omega \sim ak$ and $|\delta\tilde{\mathbf{v}}| \sim |\delta\tilde{\mathbf{b}}|$, it is possible to estimate the contribution from different terms to Eqn (58):

$$\frac{a}{c} : \frac{v}{c} : \frac{a}{c} : \frac{a^3}{c^3} : \frac{a^2 v}{c^2 c}. \quad (64)$$

In these ratios, the last two terms correspond to the contribution from the displacement current. We consider two cases. Let $v \sim a \ll c$. This corresponds to the classical nonrelativistic MHD case. Indeed, both terms related to the displacement current are small because $(v/c)^2 \ll 1$. The dispersion relation in this case takes the form

$$\omega_{\pm} = \mathbf{vk} \pm |\mathbf{ak}|. \quad (65)$$

Substituting this in (59) yields a relation between the perturbation velocity and magnetic field amplitudes:

$$\delta\tilde{v}_{\pm} = \mp \operatorname{sgn}(\mathbf{ak}) \delta\tilde{b}_{\pm}. \quad (66)$$

When $v \ll a$, only the last term in (53) related to the displacement current is negligibly small. The next-to-last term can be not small if $(a/c)^3 \gtrsim v/c$. The characteristic equation in this case becomes

$$\left(1 + \frac{a^2}{c^2}\right)\omega^2 - \left(2 + \frac{a^2}{c^2}\right)(\mathbf{vk})\omega - (\mathbf{ak})^2 + (\mathbf{vk})^2 = 0. \quad (67)$$

The dispersion relation takes the form

$$\omega_{\pm} = \left(1 - \gamma_A^2 \frac{a^2}{2c^2}\right)(\mathbf{vk}) \pm \gamma_A |\mathbf{ak}| \left[1 + \left(\gamma_A \frac{a^2}{2c^2} \frac{\mathbf{vk}}{|\mathbf{ak}|}\right)^2\right]^{1/2}, \quad (68)$$

where

$$\gamma_A = \left(1 + \frac{a^2}{c^2}\right)^{-1/2}. \quad (69)$$

Substituting the dispersion relation in (59) and using (63), we obtain a relation between perturbation amplitudes:

$$\delta\tilde{v}_{\pm} = \operatorname{sgn}(\mathbf{ak}) \left\{ \gamma_A^2 \frac{a^2}{2c^2} \frac{\mathbf{vk}}{|\mathbf{ak}|} \mp \gamma_A \left[1 + \left(\gamma_A \frac{a^2}{2c^2} \frac{\mathbf{vk}}{|\mathbf{ak}|}\right)^2\right]^{1/2} \right\} \delta\tilde{b}_{\pm}. \quad (70)$$

It can be shown that the estimate

$$\gamma_A \frac{a^2}{c^2} \left| \frac{\mathbf{vk}}{\mathbf{ak}} \right| \leq \frac{av}{c^2} \left(1 + \left| \frac{k_{\perp}}{k_{\parallel}} \right| \right). \quad (71)$$

holds in general. In the next section, we see that the ratio $|k_{\perp}/k_{\parallel}|$ can be quite large. However, in the approximation $v \ll a \sim c$, the quantity in (71) is small compared with unity. Using this, we can simplify the form of the dispersion equation and the relation between amplitudes:

$$\omega_{\pm} = \left(1 - \gamma_A^2 \frac{a^2}{2c^2}\right)(\mathbf{vk}) \pm \gamma_A |\mathbf{ak}|, \quad (72)$$

$$\delta\tilde{v}_{\pm} = \mp \operatorname{sgn}(\mathbf{ak}) \gamma_A \delta\tilde{b}_{\pm}. \quad (73)$$

It is easy to see that in the case $a \ll c$, relations (72) and (73) respectively transform into (65) and (66). In the opposite case $a \gg c$, we find

$$\omega_{\pm} = \pm |ck_{\parallel}|, \quad (74)$$

$$\delta\tilde{v}_{\pm} = \mp \operatorname{sgn}(\mathbf{ak}) \frac{c}{a} \delta\tilde{b}_{\pm}. \quad (75)$$

If the formal value of Alfvén velocity (55) is much higher than the speed of light (this can take place not only in a strong magnetic field but also in a low-density medium), velocity perturbations disappear, and magnetic field perturbations behave as they do for an electromagnetic wave in a vacuum.

We write the final form of the system of equations for Alfvén waves in the adopted approximation by assuming a slow change in the background variables and also taking the possible magnetic viscosity contribution into account. Following the estimates made above, we should omit the term proportional to the bulk gas velocity in the expression for the displacement current [the last term in Eqn (53)]. Then the displacement current effect in the Euler equation reduces to the appearance of a relativistic correction to the acceleration component orthogonal to the background field:

$$\frac{1}{4\pi\rho c} \frac{\partial \delta^{(1)}\mathbf{E}}{\partial t} \times \mathbf{B} = \frac{a^2}{c^2} (\hat{\mathbf{I}} - \mathbf{e}_{\parallel} \otimes \mathbf{e}_{\parallel}) \frac{\partial \delta\mathbf{v}}{\partial t}. \quad (76)$$

In the case of Alfvén waves on a homogeneous background, Euler equation (53) constrains only the transverse perturbation components. This remains valid if a slow variation of the background variables is required. Thus, with account for (61) and (76), the system of equations for Alfvén perturbations on an inhomogeneous background takes the form

$$\gamma_A^{-2} \frac{\partial \delta\mathbf{v}}{\partial t} + (\mathbf{v}\nabla) \delta\mathbf{v} + (\delta\mathbf{v}\nabla) \mathbf{v} + \delta\mathbf{b} \times \operatorname{rot} \mathbf{a} - (\mathbf{a}\nabla) \delta\mathbf{b} = 0, \quad (77)$$

$$\frac{\partial \delta\mathbf{b}}{\partial t} + (\mathbf{v}\nabla) \delta\mathbf{b} - (\mathbf{a}\nabla) \delta\mathbf{v} + (\delta\mathbf{v}\nabla) \mathbf{a} - (\delta\mathbf{b}\nabla) \mathbf{v} + (\nabla\mathbf{v}) \delta\mathbf{b} + \operatorname{rot}(\eta \operatorname{rot} \delta\mathbf{b}) = 0. \quad (78)$$

Equations for Fourier harmonics (72) and (73) respectively correspond to these equations.

3.2 Double correlators

Turbulent sources in Eqns (50)–(52) are double correlation functions (correlators) of perturbations. We represent the correlators in the form of decomposition into spatial Fourier harmonics:

$$\delta f(\mathbf{x}) \delta g(\mathbf{x}) = \int d^3 p \int d^3 q \exp[i(\mathbf{p} + \mathbf{q})\mathbf{x}] \delta\tilde{f}_{\mathbf{p}} \delta\tilde{g}_{\mathbf{q}}. \quad (79)$$

We assume that the perturbation modes form a statistical ensemble, with modes with different wave numbers being mutually uncorrelated. The correlation function of modes in the Fourier space is then expressed in terms of the spectral density or the power spectrum, denoted as $\langle \delta\tilde{f} \delta\tilde{g} \rangle$:

$$\langle \delta\tilde{f}_{\mathbf{p}} \delta\tilde{g}_{\mathbf{q}} \rangle = \delta(\mathbf{p} + \mathbf{q}) \langle \delta\tilde{f} \delta\tilde{g} \rangle_{\mathbf{p}}. \quad (80)$$

The correlation coefficient of the fields δf and δg at a point \mathbf{x} can also be expressed in terms of the power spectrum:

$$\langle \delta f(\mathbf{x}) \delta g(\mathbf{x}) \rangle = \int d^3 k \langle \delta\tilde{f} \delta\tilde{g} \rangle_{\mathbf{k}}. \quad (81)$$

If the power spectra of correlation functions are known, they can be used to directly calculate the sources in Eqns (50)–(52). However, the accuracy of calculating sources in this way can be insufficient if the power spectra were obtained in an inherently rough approximation. In this case, to compute the sources, we can use the equation for

small Alfvén perturbations. For this, we write the relations for double correlators:

$$\frac{\partial}{\partial t} \langle \delta \mathbf{v} \otimes \delta \mathbf{v} \rangle = \frac{\partial \delta \mathbf{v}}{\partial t} \otimes \delta \mathbf{v} + \delta \mathbf{v} \otimes \frac{\partial \delta \mathbf{v}}{\partial t}. \quad (82)$$

The time derivative here should be substituted from Eqn (77). After averaging, linear combinations of double correlators of the velocity perturbation components and the magnetic field, as well as cross correlators, appear in the right-hand side. Equations for $\langle \delta \mathbf{b} \otimes \delta \mathbf{b} \rangle$ and $\langle \delta \mathbf{v} \otimes \delta \mathbf{b} \rangle$ can be derived similarly. In the coordinate representation in Cartesian coordinates, evolutionary equations for the spectral powers of double correlators have the form (we omit indices besides those designating Cartesian components of vectors)

$$\frac{\partial}{\partial t} \langle \delta \tilde{v}_i \delta \tilde{v}_j \rangle = -i\gamma_A^2 (\mathbf{v}\mathbf{k}) \langle \delta \tilde{v}_i \delta \tilde{v}_j \rangle - \gamma_A^2 (\nabla_{\parallel} v_i) \langle \delta \tilde{v}_i \delta \tilde{v}_j \rangle + \gamma_A^2 \varepsilon_{ilm} (\text{rot } \mathbf{a})_l \langle \delta \tilde{b}_m \delta \tilde{v}_j \rangle + i\gamma_A^2 (\mathbf{a}\mathbf{k}) \langle \delta \tilde{b}_i \delta \tilde{v}_j \rangle + (i \leftrightarrow j), \quad (83)$$

$$\begin{aligned} \frac{\partial}{\partial t} \langle \delta \tilde{v}_i \delta \tilde{b}_j \rangle &= -2i\gamma_A^2 (\mathbf{v}\mathbf{k}) \langle \delta \tilde{v}_i \delta \tilde{b}_j \rangle - \gamma_A^2 (\nabla_{\parallel} v_i) \langle \delta \tilde{v}_i \delta \tilde{b}_j \rangle \\ &+ \gamma_A^2 \varepsilon_{ilm} (\text{rot } \mathbf{a})_l \langle \delta \tilde{b}_m \delta \tilde{b}_j \rangle + i\gamma_A^2 (\mathbf{a}\mathbf{k}) \langle \delta \tilde{b}_i \delta \tilde{b}_j \rangle \\ &+ i(\mathbf{a}\mathbf{k}) \langle \delta \tilde{v}_i \delta \tilde{v}_j \rangle - (\nabla_{\parallel} a_j) \langle \delta \tilde{v}_i \delta \tilde{v}_l \rangle + (\nabla_{\parallel} v_j) \langle \delta \tilde{v}_i \delta \tilde{b}_l \rangle \\ &- (\nabla_{\parallel} \mathbf{v}) \langle \delta \tilde{v}_i \delta \tilde{b}_j \rangle - \eta k^2 \langle \delta \tilde{v}_i \delta \tilde{b}_j \rangle, \end{aligned} \quad (84)$$

$$\begin{aligned} \frac{\partial}{\partial t} \langle \delta \tilde{b}_i \delta \tilde{b}_j \rangle &= -i(\mathbf{v}\mathbf{k}) \langle \delta \tilde{b}_i \delta \tilde{b}_j \rangle + i(\mathbf{a}\mathbf{k}) \langle \delta \tilde{v}_i \delta \tilde{b}_j \rangle \\ &- (\nabla_{\parallel} a_i) \langle \delta \tilde{v}_j \delta \tilde{b}_j \rangle + (\nabla_{\parallel} v_i) \langle \delta \tilde{b}_l \delta \tilde{b}_j \rangle - (\nabla_{\parallel} \mathbf{v}) \langle \delta \tilde{b}_i \delta \tilde{b}_j \rangle \\ &- \eta k^2 \langle \delta \tilde{b}_i \delta \tilde{b}_j \rangle + (i \leftrightarrow j). \end{aligned} \quad (85)$$

Here, ε_{ilm} is the Levi-Civita symbol, $(\text{rot } \mathbf{a})_l = \varepsilon_{lij} \nabla_j a_j$, and $k^2 = k_{\parallel}^2 + k_{\perp}^2$. The symbols $(i \leftrightarrow j)$ denote permutation of indices i and j .

Instead of directly solving system of equations (83)–(85), we use the iteration procedure. We write this system of equations in the form

$$\frac{dC_{\alpha}}{dt} = \sum_{\beta} U_{\alpha\beta} C_{\beta}, \quad (86)$$

where C_{α} are double correlators and $U_{\alpha\beta}$ is the matrix of system (83)–(85). We assume that the right-hand side of this equation causes relaxation of the system to some equilibrium state $C^{(0)}$ over a characteristic time τ . At the same time, perturbations can take the system away from equilibrium. Small deviations from equilibrium can be described in the framework of the so-called τ -approximation:

$$\sum_{\beta} U_{\alpha\beta} C_{\beta}^{(0)} = \frac{C_{\alpha} - C_{\alpha}^{(0)}}{\tau}. \quad (87)$$

Hence,

$$C_{\alpha} = C_{\alpha}^{(0)} + \tau \sum_{\beta} U_{\alpha\beta} C_{\beta}^{(0)}. \quad (88)$$

Repeating substitutions like (88) in Eqn (86), we can obtain higher-order corrections in the relaxation time to the equilibrium solution $C_{\alpha}^{(0)}$.

The characteristic relaxation time can be defined as the inverse of the maximum-modulus eigenvalue of the matrix $U_{\alpha\beta}$. We rewrite system (83)–(85) by ignoring the background

flow velocity and background variables gradients:

$$\frac{\partial}{\partial t} \langle \delta \tilde{v}^2 \rangle = 2i\gamma_A^2 a k_{\parallel} \langle \delta \tilde{v} \delta \tilde{b} \rangle, \quad (89)$$

$$\frac{\partial}{\partial t} \langle \delta \tilde{v} \delta \tilde{b} \rangle = i a k_{\parallel} \langle \delta \tilde{v}^2 \rangle + i\gamma_A^2 a k_{\parallel} \langle \delta \tilde{b}^2 \rangle - \eta k^2 \langle \delta \tilde{v} \delta \tilde{b} \rangle, \quad (90)$$

$$\frac{\partial}{\partial t} \langle \delta \tilde{b}^2 \rangle = 2i a k_{\parallel} \langle \delta \tilde{v} \delta \tilde{b} \rangle - 2\eta k^2 \langle \delta \tilde{b}^2 \rangle. \quad (91)$$

The matrix of this system has three eigenvalues:

$$\frac{1}{\tau_0} = -\eta k^2, \quad (92)$$

$$\frac{1}{\tau_{\pm}} = \frac{1}{\tau_0} \pm (\eta^2 k^4 - 4\gamma_A^2 a^2 k_{\parallel}^2)^{1/2} \quad (93)$$

(the signs \pm in these formulas must not be confused with the propagation directions of Alfvén waves). At $k = 0$, all eigenvalues vanish. If $k \rightarrow \infty$ or $a k_{\parallel} \rightarrow 0$, we have

$$\frac{1}{\tau_{-}} = -2\eta k^2, \quad \frac{1}{\tau_{+}} = 0. \quad (94)$$

It is easy to see that the solutions always relax, with the fastest relaxation occurring for the solution of the τ_{-} branch. Indeed, when the expression in the radicand in (93) is positive, we have

$$\frac{1}{\tau_{-}} \leq \frac{1}{\tau_0} \leq \frac{1}{\tau_{+}} < 0. \quad (95)$$

Otherwise,

$$\text{Re} \left(\frac{1}{\tau_{-}} \right) = \text{Re} \left(\frac{1}{\tau_{+}} \right) = \frac{1}{\tau_0} < 0, \quad (96)$$

where $\text{Re}(z)$ denotes the real part of a complex number z .

The expression for eigenvalues (93) suggests that the relaxation has two regimes: the *Alfvén* one, with the characteristic time of the order of $|\gamma_A a k_{\parallel}|^{-1}$, and the *dissipative* one, with the characteristic time of the order of $(\eta k^2)^{-1}$. We define the characteristic relaxation time in the τ -approximation in the form

$$\tau = \min(\tau_A, \tau_d), \quad (97)$$

where we let

$$\tau_A = \frac{1}{|\gamma_A a k_{\parallel}|} \quad (98)$$

denote the Alfvén time and assume the approximate dissipation time to be

$$\tau_d = \frac{1}{2\eta k^2}. \quad (99)$$

Besides the dissipation relaxation regime, Ohmic dissipation determines the smallest transverse spatial scale for Alfvén waves:

$$\lambda_{\min} = \frac{4\eta}{\gamma_A a}. \quad (100)$$

Indeed, it can be shown that for waves with transverse wave numbers satisfying $k_{\perp} > \lambda_{\min}^{-1}$, the eigenvalues in (93) are real

and negative. This means that such waves only decay without oscillations. In the limit of a very high Alfvén velocity, $a \gg c$, the smallest transverse scale of Alfvén waves tends to $4\eta/c$.

3.3 Power spectrum

Turbulent sources in Eqns (50)–(52) contain quadratic dependences on the amplitudes of perturbations and are expressed in terms of double correlation functions of the components of velocity and magnetic field perturbations, as well as their products. In Section 3.2, we have shown how the double correlation functions can be calculated taking non-equilibrium effects into account. In this section, we formulate expressions for equilibrium correlators based on the theory of Alfvén wave turbulence presented in [24].

Each wave vector is associated with a pair of Alfvén waves traveling along the background magnetic field in opposite directions (see Section 3.1). If we assume that waves running in different directions and with different wave vectors do not mutually correlate, then, with (63) and (73), we can write the spectral density of correlation tensors of perturbations $\delta\mathbf{b}$ and $\delta\mathbf{v}$ in the form

$$\langle \delta\tilde{\mathbf{b}} \otimes \delta\tilde{\mathbf{b}} \rangle_{\pm} = \mathbf{e}_n \otimes \mathbf{e}_n \langle \delta\tilde{b}^2 \rangle_{\pm}, \quad (101)$$

$$\langle \delta\tilde{\mathbf{v}} \otimes \delta\tilde{\mathbf{v}} \rangle_{\pm} = \mathbf{e}_n \otimes \mathbf{e}_n \gamma_A^2 \langle \delta\tilde{b}^2 \rangle_{\pm}, \quad (102)$$

$$\langle \delta\tilde{\mathbf{v}} \otimes \delta\tilde{\mathbf{b}} \rangle_{\pm} = \mp \operatorname{sgn}(k_{\parallel}) \mathbf{e}_n \otimes \mathbf{e}_n \gamma_A \langle \delta\tilde{b}^2 \rangle_{\pm}. \quad (103)$$

We note that these tensors have nonzero components only in the plane orthogonal to the Alfvén velocity vector. Expressions (101)–(103) contain the same quantity $\langle \delta\tilde{b}^2 \rangle_{\pm}$, which we call the power spectrum and for which we introduce the notation

$$P_{\pm}(\mathbf{k}) = \langle \delta\tilde{b}^2 \rangle_{\pm}. \quad (104)$$

The energy flux is associated with Alfvén waves. The corresponding Poynting vector can be written as

$$\frac{\delta\mathbf{S}}{\rho} = \frac{c}{4\pi\rho} \delta^{(1)}\mathbf{E} \times \mathbf{B} + \frac{c}{4\pi\rho} \delta^{(1)}\mathbf{E} \times \delta\mathbf{B} + \frac{c}{4\pi\rho} \delta^{(2)}\mathbf{E} \times \mathbf{B}. \quad (105)$$

Only the second term in the right-hand side of (105) makes a nonzero contribution to the energy flux after averaging over the mode ensemble. Indeed, the mean of the first linear term is zero. The third term contains the vector square of \mathbf{e}_n and also vanishes. In the Fourier representation, the mean energy flux transferred by Alfvén waves with a wave vector \mathbf{k} is

$$\frac{\langle \delta\tilde{\mathbf{S}} \rangle_{\pm}}{\rho} = -\langle (\delta\tilde{\mathbf{v}}_{\pm} \times \mathbf{a}) \times \delta\tilde{\mathbf{b}}_{\pm} \rangle = \pm \operatorname{sgn}(k_{\parallel}) \gamma_A \mathbf{a} P_{\pm}(\mathbf{k}). \quad (106)$$

The dispersion relation for Alfvén waves in Eqn (72) has two branches corresponding to the opposite directions of the phase velocity. Here, the mutual orientation of the amplitude of the velocity perturbations and magnetic field (73) also depends on the wave vector orientation relative to the background field direction. Possible types of Alfvén waves are listed in Table 1. It is seen that for a given mutual orientation of $\delta\tilde{\mathbf{v}}_{\pm}$ and $\delta\tilde{\mathbf{b}}_{\pm}$, only one orientation of the wave vector and one direction of energy propagation is possible.

Nonlinear equations of Alfvén wave turbulence were formulated and solved in [24] in terms of the Elsasser variables $\mathbf{z}^{\pm} = \delta\mathbf{v} \pm \delta\mathbf{b}$. In such an approach, the same wave vector is associated with a pair of waves that differ by the mutual orientation of the velocity and magnetic field

Table 1. Types of Alfvén waves.

	$k_{\parallel} > 0$	$k_{\parallel} < 0$
$\delta\tilde{\mathbf{v}}_+ \uparrow\uparrow \delta\tilde{\mathbf{b}}_+$	—	$\delta S_{\parallel,+} < 0$
$\delta\tilde{\mathbf{v}}_+ \uparrow\downarrow \delta\tilde{\mathbf{b}}_+$	$\delta S_{\parallel,+} > 0$	—
$\delta\tilde{\mathbf{v}}_- \uparrow\uparrow \delta\tilde{\mathbf{b}}_-$	$\delta S_{\parallel,-} < 0$	—
$\delta\tilde{\mathbf{v}}_- \uparrow\downarrow \delta\tilde{\mathbf{b}}_-$	—	$\delta S_{\parallel,-} > 0$

perturbation amplitudes and hence by the energy flux direction. We let the energy power spectrum in the Elsasser variables be denoted as¹

$$\Pi^{\pm}(\mathbf{k}) = \frac{\langle (\tilde{\mathbf{z}}^{\pm})^2 \rangle}{2}. \quad (107)$$

As shown in [24], the universal character of the energy spectrum in Alfvén wave turbulence appears only for the energy spectrum part depending on the transverse wave numbers k_{\perp} , while the longitudinal part of the spectrum (depending on k_{\parallel}) is determined by external conditions and enters the wave turbulence equations only as a parameter. These properties of the energy spectrum are due to the Alfvén wave turbulence in a strong magnetic field redistributing energy in the directions perpendicular to the background field. As a result, the energy spectrum of Alfvén turbulence takes the form

$$\Pi^{\pm}(k_{\parallel}, k_{\perp}) = f(k_{\parallel}) \Pi_{\perp}^{\pm}(k_{\perp}), \quad (108)$$

where $f(k_{\parallel})$ is an arbitrary dimensionless function of the longitudinal wave vector component satisfying the condition $f(0) = 1$, i.e., $\Pi_{\perp}^{\pm}(k_{\perp}) = \Pi^{\pm}(k_{\parallel} = 0, k_{\perp})$, where Π_{\perp}^{\pm} is the transverse part of the energy spectrum. Below, following the notation in [24], we write the transverse energy power spectrum as

$$E_{\perp}^{\pm}(k_{\perp}) = 2\pi k_{\perp} \Pi_{\perp}^{\pm}(k_{\perp}). \quad (109)$$

According to Table 1, in the Elsasser variables, waves with opposite signs transfer energy in opposite directions; no distinction is made between different branches of the dispersion relation (the lower sign \pm at the amplitude vectors). The formalism in [24] can be made consistent with the definitions adopted here if the power spectrum is

$$P_{\pm}(\mathbf{k}) = \frac{f(k_{\parallel})}{2\pi k_{\perp}} \begin{cases} E_{\perp}^{\pm}(k_{\perp}), & k_{\parallel} > 0, \\ E_{\perp}^{\mp}(k_{\perp}), & k_{\parallel} < 0. \end{cases} \quad (110)$$

It is shown in [24] that as turbulence sets in, the inertial interval forms, inside which the energy spectrum has a power-law dependence on the transverse wave number:²

$$E_{\perp}^{\pm}(k_{\perp}) \propto k_{\perp}^{n_{\pm}}. \quad (111)$$

The spectral exponents are in the range $-3 < n_{\pm} < -1$ and are related as $n_+ + n_- = -4$.

It follows from (111) that waves with different signs can form energy cascades with different exponents. The

¹ In [24] the power spectrum is denoted by e^{\pm} .

² In comparison with formulas (63) and (64) from [24], this expression does not contain a small parameter in linearized MHD equations because it is assumed to be included in the total turbulent energy.

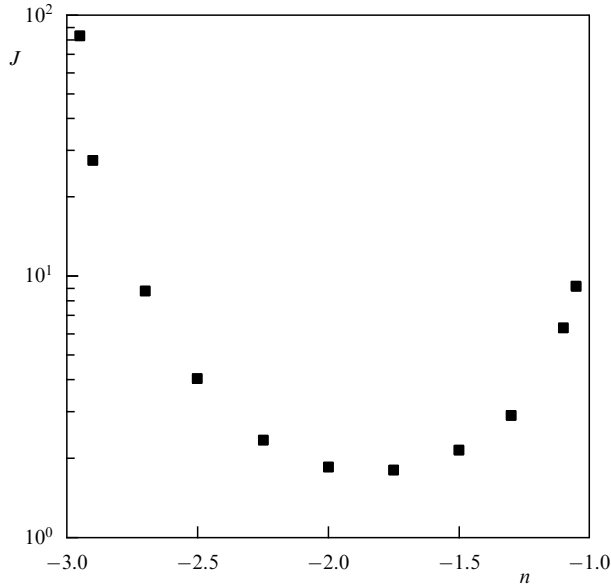


Figure 1. Normalized factor $J(n)$ in the energy spectrum as a function of the spectral exponent.

energy flux along and across the background field can also be different in general. The case of a balanced spectrum is interesting, where the total energy flux vanishes, $\langle \delta \mathbf{S}_+ \rangle + \langle \delta \mathbf{S}_- \rangle = 0$, and the spectral exponents are $n_+ = n_- = -2$. In this case, the energy spectrum takes the form [24]

$$E_{\perp}(k_{\perp}) = E_{\perp}^+(k_{\perp}) = E_{\perp}^-(k_{\perp}) = \left(\frac{2\epsilon a}{\pi J(-2)} \right)^{1/2} k_{\perp}^{-2}, \quad (112)$$

where ϵ is the energy flux through the inertial interval.³ The variable J in the denominator of this expression depends on the spectral exponent and can be found from the kinetic equation for Alfvén wave turbulence [24]:

$$J(n) = 2^{n+3} \int_1^{\infty} dx \int_{-1}^1 dy \frac{\sqrt{(x^2-1)(1-y^2)}(xy+1)^2}{(x-y)^{n+6}(x+y)^{2-n}} \times [(x+y)^{1-n} - 2^{1-n}] \ln \left(\frac{x+y}{2} \right). \quad (113)$$

This integral converges for $-3 < n < -1$. The plot of $J(n)$ is presented in Fig. 1. For the balanced spectrum, $J(-2) = 1.86$ and

$$E_{\perp}(k_{\perp}) \approx 0.59 \sqrt{\epsilon a} k_{\perp}^{-2}. \quad (114)$$

The longitudinal part of the spectrum is independent of the external conditions. It should be remembered, however, that $k_{\perp} \gg k_{\parallel}$ is assumed in the wave turbulence approximation in which solution (111) was obtained. In addition, the longitudinal part of the spectrum is restricted by the condition $f(k_{\parallel} = 0) = 1$. Introducing the characteristic longitudinal scale for the magnetic configuration, L_{\parallel} , we can use the approximate expression

$$f(k_{\parallel}) = h(1 - |k_{\parallel} L_{\parallel}|), \quad (115)$$

³ Here and below, the factor ϵ does not coincide with that introduced in Section 2.1. These factors differ by the dimension of length.

where $h(x)$ is the Heaviside function equal to 0 for $x < 0$ and 1 otherwise.

Using definitions (101), (102), (110), and (112), we can find the magnetic energy of wave turbulence per unit mass

$$\frac{\langle |\delta \mathbf{b}|^2 \rangle}{2} = \frac{W}{2}, \quad (116)$$

and the kinetic energy

$$\frac{\langle |\delta \mathbf{v}|^2 \rangle}{2} = \gamma_A^2 \frac{W}{2}. \quad (117)$$

The quantity W is defined such that it is equal to the total (magnetic and kinetic) energy of turbulence in the weak-field limit $a \ll c$:

$$W = W_+ + W_-, \quad (118)$$

where W_{\pm} is the total energy of waves traveling along and against the background field:

$$W_{\pm} = \int d^3k P_{\pm}(\mathbf{k}) = \frac{2}{L_{\parallel}} \int_{L_{\perp}^{-1}}^{\infty} dk_{\perp} E_{\perp}(k_{\perp}) \approx 1.17 \sqrt{\epsilon a} \frac{L_{\perp}}{L_{\parallel}}. \quad (119)$$

Hence,

$$W \approx 2.34 \sqrt{\epsilon a} \frac{L_{\perp}}{L_{\parallel}}. \quad (120)$$

The vector of energy flux density per unit mass is defined by the difference between energies in dispersion branches:

$$\frac{\langle \delta \mathbf{S} \rangle}{\rho} = \frac{\langle \delta \mathbf{S} \rangle_+ + \langle \delta \mathbf{S} \rangle_-}{\rho}, \quad (121)$$

where, according to (106), (112), and (119),

$$\frac{\langle \delta \mathbf{S} \rangle_{\pm}}{\rho} = \pm \gamma_A \mathbf{a} W_{\pm}. \quad (122)$$

Thus, in the case of a balanced spectrum, the energy flux along the background magnetic field vanishes.

As noted in Section 3.1, in the limit of a high Alfvén velocity, the velocity perturbation amplitudes tend to zero as c/a , and therefore the kinetic energy decreases as c^2/a^2 . We note that expression (117) has no relativistic covariant form and can be used, strictly speaking, only under the condition

$$\frac{\gamma_A^2 W}{c^2} \ll 1. \quad (123)$$

The direct substitution of the expression for W straightforwardly shows that the left-hand side of this inequality attains a maximum at $a = c/\sqrt{3}$; therefore, if the inequality holds at this Alfvén velocity, it must hold for any value of the Alfvén velocity with other parameters fixed.

4. Sources

The general expression for the double correlation function includes the unperturbed part and the correction emerging in the τ -approximation (see Section 3.2):

$$\langle \delta f \delta g \rangle = \langle \delta f \delta g \rangle^{(0)} + \langle \delta f \delta g \rangle^{(1)}, \quad (124)$$

where

$$\langle \delta f \delta g \rangle^{(0)} = \sum_{\pm} \int d^3 k \langle \delta \tilde{f} \delta \tilde{g} \rangle_{\pm}, \quad (125)$$

$$\langle \delta f \delta g \rangle^{(1)} = \sum_{\pm} \int d^3 k \tau(\mathbf{k}) \frac{\partial}{\partial t} \langle \delta \tilde{f} \delta \tilde{g} \rangle_{\pm}. \quad (126)$$

The unperturbed part of (124) is determined only by power spectrum (110). At the same time, the τ -correction is defined by the right-hand side of Eqns (83)–(85) for the corresponding spectral density and can depend on the background magnetic field and its gradients. Below, we take only those terms in the right-hand sides of (83)–(85) into account that make an isotropic contribution to integral (126) over the transverse wave numbers. In addition, we neglect the τ -correction if the unperturbed part is nonzero.

In our case, there are two fundamentally different relaxation regimes: diffusion and Alfvén. In the first case, the relaxation time is the characteristic diffusion time $\tau_d = [2\eta(k_{\parallel}^2 + k_{\perp}^2)]^{-1}$. In the second case, the relaxation time is the Alfvén time $\tau_A = |\gamma_A a k_{\parallel}|^{-1}$ and depends on the background magnetic field. Depending on the problem parameters, either the diffusion or the Alfvén relaxation regime can dominate in the integration domain in expression (126).

We consider the scale hierarchy of the problem:

$$k_{\parallel} < L_{\parallel}^{-1} \ll L_{\perp}^{-1} < k_{\perp} < \lambda^{-1} \lesssim \lambda_{\min}^{-1}, \quad (127)$$

where λ is the turbulence dissipation scale (it is defined rigorously in Section 4.2), and λ_{\min} is the minimum possible Alfvén wavelength (100). We introduce dimensionless variables as the ratios of some characteristic scales:

$$\alpha = \left(\frac{\lambda_{\min}}{2L_{\parallel}} \right)^{1/2} = \left(\frac{2\eta}{\gamma_A a L_{\parallel}} \right)^{1/2}, \quad (128)$$

$$\beta = \frac{L_{\perp}}{L_{\parallel}}. \quad (129)$$

It can be shown that the following relations hold:

$$\alpha^2 \lesssim \frac{\lambda}{L_{\parallel}} < \frac{1}{L_{\parallel} k_{\perp}} < \beta \ll 1 < \frac{1}{L_{\parallel} k_{\parallel}}. \quad (130)$$

Figure 2 shows the location of domains corresponding to different relaxation regimes on the wavenumber plane. The rectangles show the possible integration boundaries. It is seen that a decrease in the background field strength (increase in α) can lead to the diffusion relaxation only. Indeed, the condition of the Alfvén relaxation regime can be written as

$$2\eta(k_{\parallel}^2 + k_{\perp}^2) < \gamma_A a k_{\parallel} \quad (131)$$

or

$$(\alpha^2 L_{\parallel} k_{\parallel})^2 + (\alpha^2 L_{\parallel} k_{\perp})^2 < \alpha^2 L_{\parallel} k_{\parallel}. \quad (132)$$

For the wave number domain where $\tau_A < \tau_d$ to fall within the integration limits, it is sufficient that inequality (132) hold for $k_{\parallel} = L_{\parallel}^{-1}$ and $k_{\perp} = L_{\perp}^{-1}$:

$$\alpha^2 < \frac{\beta^2}{\beta^2 + 1}. \quad (133)$$

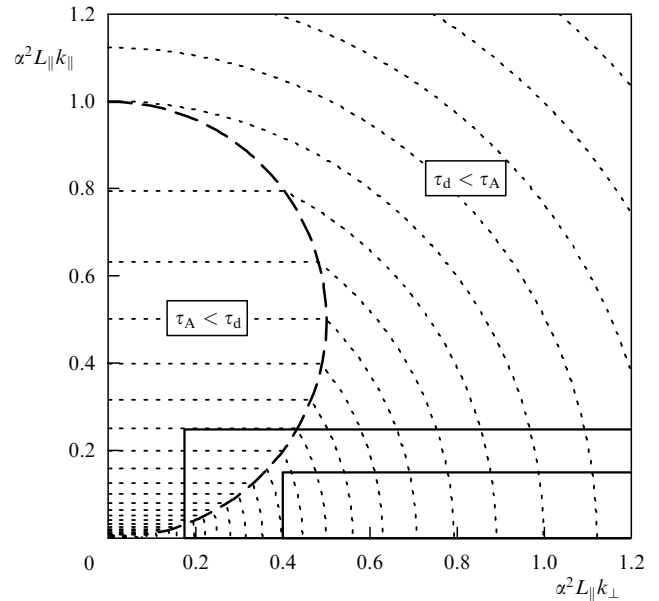


Figure 2. Relaxation regime of Alfvén turbulence on the wavenumber plane. Thin dashed lines show the relaxation time isochrones, with the lines close to the coordinate origin corresponding to longer times. The long-dashed line separates regions with different relaxation regimes. The rectangles show integration domains for $\alpha < \beta$ (larger rectangle) and $\alpha > \beta$ (smaller rectangle).

With (130), this condition can be approximately stated as

$$\alpha < \beta. \quad (134)$$

If $\alpha > \beta$, only the diffusion relaxation is realized. This condition can be rewritten in the form $2\eta L_{\parallel} > \gamma_A a L_{\perp}^2$; therefore, the diffusion regime occurs at low Alfvén velocities and/or on a small transverse turbulence scale.

4.1 Turbulent pressure and stresses

According to definition (101), components of the magnetic stress tensor are nonzero only in the directions transverse to the background magnetic field. The projection of this tensor onto the plane orthogonal to \mathbf{e}_{\parallel} is obviously independent of the direction in this plane. Moreover, the stress tensor and pressure (per unit mass) are obviously related as

$$\langle |\delta \mathbf{b}|^2 \rangle = \text{tr} \langle \delta \mathbf{b} \otimes \delta \mathbf{b} \rangle. \quad (135)$$

Hence, using (116), we obtain

$$\langle \delta \mathbf{b} \otimes \delta \mathbf{b} \rangle = \hat{\mathbf{T}} \frac{W}{2}, \quad (136)$$

where $\hat{\mathbf{T}}$ is the projection operator on the plane orthogonal to the background field direction \mathbf{e}_{\parallel} :

$$\hat{\mathbf{T}} = \hat{\mathbf{I}} - \mathbf{e}_{\parallel} \otimes \mathbf{e}_{\parallel}. \quad (137)$$

It is seen that the magnetic stress tensor has only the longitudinal component:

$$\rho \left(\hat{\mathbf{I}} \frac{\langle |\delta \mathbf{b}|^2 \rangle}{2} - \langle \delta \mathbf{b} \otimes \delta \mathbf{b} \rangle \right) = \mathbf{e}_{\parallel} \otimes \mathbf{e}_{\parallel} \frac{\rho W}{2}. \quad (138)$$

In a similar way, using (102), we can calculate the stress tensor due to velocity perturbations:

$$\rho \langle \delta \mathbf{v} \otimes \delta \mathbf{v} \rangle = \hat{\mathbf{T}} \frac{\rho \gamma_A^2 W}{2}. \quad (139)$$

Thus, the total turbulent stress tensor has both longitudinal and transverse components:

$$\rho \left(\hat{\mathbf{T}} \frac{\langle |\delta \mathbf{b}|^2 \rangle}{2} - \langle \delta \mathbf{b} \otimes \delta \mathbf{b} \rangle + \langle \delta \mathbf{v} \otimes \delta \mathbf{v} \rangle \right) = \left(\hat{\mathbf{T}} - \frac{\gamma_A^2 a^2}{c^2} \hat{\mathbf{T}} \right) \frac{\rho W}{2}. \quad (140)$$

In a weak field ($a \ll c$), the tensor takes an isotropic form, and in a strong field ($a \gg c$), only the longitudinal component survives.

4.2 Turbulent viscosity

The turbulent source in the induction equation vanishes in the zeroth order of the τ -approximation. Indeed, we can write

$$\langle \delta \mathbf{v} \times \delta \mathbf{b} \rangle^{(0)} = \gamma_A \sum_{\pm} (\mp 1) \int d^3 k \operatorname{sgn}(k_{\parallel}) \mathbf{e}_n \times \mathbf{e}_n P_{\pm}. \quad (141)$$

Clearly, this quantity vanishes. In the first order of the τ -approximation, only one term in the right-hand side of (84) is potentially nonzero:

$$\langle \delta \mathbf{v} \times \delta \mathbf{b} \rangle^{(1)} = \gamma_A^2 \sum_{\pm} \int d^3 k \mathbf{e}_n \times (\mathbf{e}_n \times \operatorname{rot} \mathbf{a}) \tau P_{\pm}. \quad (142)$$

This integral can be easily transformed to

$$\langle \delta \mathbf{v} \times \delta \mathbf{b} \rangle^{(1)} = -\eta_w \hat{\mathbf{T}} \operatorname{rot} \mathbf{a}, \quad (143)$$

where

$$\eta_w = \gamma_A^2 \sum_{\pm} \int d^3 k \tau P_{\pm}. \quad (144)$$

The factor η_w should be interpreted as the magnetic viscosity coefficient due to wave turbulence. Clearly, the turbulent viscosity effects appear only in the directions orthogonal to the background magnetic field.

Depending on the relation between the scales and the Alfvén velocity, the turbulent magnetic viscosity can be determined by either the diffusion or the Alfvén relaxation regime. The calculation of integral (144) in the general case yields

$$\begin{aligned} \eta_w &= 2\gamma_A^2 \int_{-L_{\parallel}^{-1}}^{L_{\parallel}^{-1}} dk_{\parallel} \int_{L_{\perp}^{-1}}^{\infty} dk_{\perp} \tau E_{\perp} \\ &= \frac{\gamma_A^2}{2\eta} W L_{\parallel}^2 \hat{\alpha}^2 \left[\frac{1}{3} + \frac{\alpha^2}{\hat{\alpha}^2} \left(\ln \frac{\beta^2}{\hat{\alpha}^2} + \frac{4}{3} \frac{\alpha}{\beta} - \frac{4}{3} \frac{\alpha}{\hat{\alpha}} \right) \right], \end{aligned} \quad (145)$$

where $\hat{\alpha} = \min(\alpha, \beta)$ [see notation (128), (129)]. In the diffusion relaxation regime $\alpha > \beta$, setting $\hat{\alpha} = \beta$ gives

$$\eta_w = \gamma_A^2 \frac{L_{\perp}^2}{6\eta} W. \quad (146)$$

For a strong Alfvén regime $\alpha \ll \beta$, we have

$$\eta_w = \frac{\gamma_A W L_{\parallel}}{a} \ln \left(\frac{\gamma_A a L_{\perp}^2}{2\eta L_{\parallel}} \right). \quad (147)$$

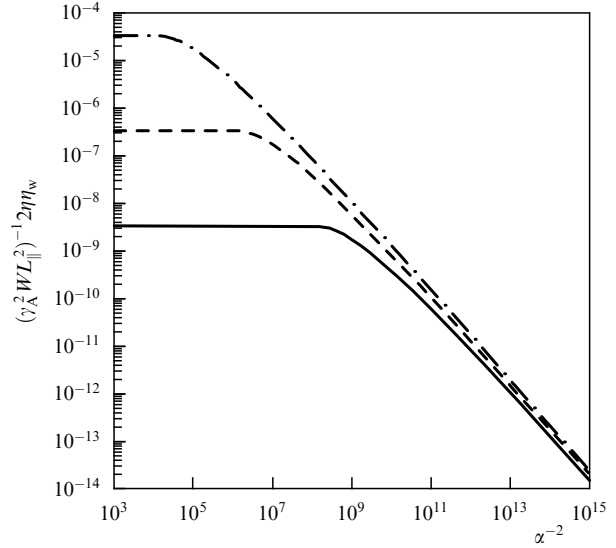


Figure 3. Magnetic turbulent viscosity coefficient as a function of the background magnetic field ($\alpha^{-2} \propto a$) for different scale ratios β : $\beta = 10^{-4}$ (solid line), $\beta = 10^{-3}$ (dashed line), and $\beta = 10^{-2}$ (dashed-dotted line).

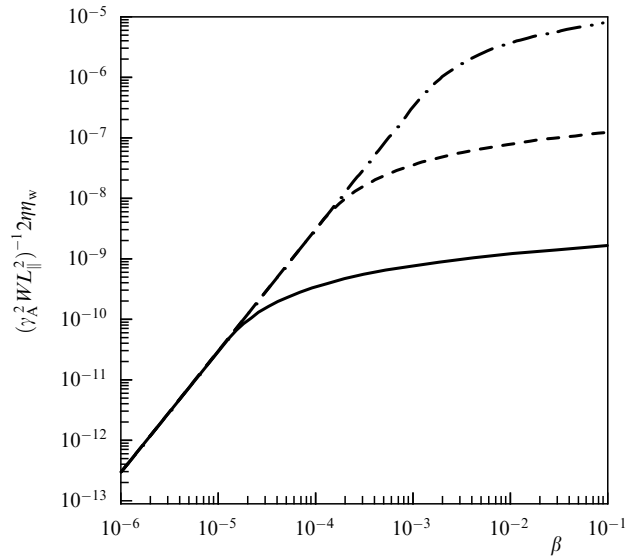


Figure 4. Magnetic turbulent viscosity coefficient as a function of the pumping scale β for different values of the parameter α : $\alpha = 10^{-5}$ (solid line), $\alpha = 10^{-4}$ (dashed line), and $\alpha = 10^{-3}$ (dashed-dotted line).

The form of the turbulent viscosity can also be obtained from physical considerations, because it is determined by the turbulent energy and the relaxation time: $\eta_w \sim W\tau$. In the diffusion regime, the relaxation time is independent of the background field strength, and the viscosity coefficient grows with the turbulence energy (which depends on the field as $W \propto B^{1/2}$). In the Alfvén regime, the relaxation time decreases with the background field strength. This weakens nonequilibrium effects [see expression (88)] and hence decreases the viscosity coefficient.

Figure 3 shows the plots of the magnetic turbulence viscosity (in dimensionless variables) as a function of $\alpha^{-2} \propto a$. The plots demonstrate that in weak fields (at large α), the dimensionless viscosity coefficient is independent of the field strength, which corresponds to the diffusion relaxation regime. The dependence of the viscosity coefficient on the pumping scale for different field strengths is shown in Fig. 4.

At small pumping scales ($\beta \rightarrow 0$), the diffusion relaxation regime with a quadratic dependence on scale always occurs. At large pumping scales, the viscosity coefficient increases logarithmically.

The dissipation scale determines the smallest turbulence scale or the lower inertial interval boundary. It can be defined as the scale λ at which the turbulent viscosity equals the microscopic one. We use expression (146) for the turbulent viscosity in the diffusion relaxation regime, which is valid in the small-scale limit:

$$\eta_w = \frac{2.34}{6} \frac{\gamma_A^2 (\epsilon a)^{1/2}}{\eta} \frac{L_\perp^3}{L_\parallel}. \quad (148)$$

Here, we have expressed the turbulent energy in terms of the flux in accordance with definition (120). On the dissipation scale, we have

$$\eta = \frac{2.34}{6} \frac{\gamma_A^2 (\epsilon a)^{1/2}}{\eta} \frac{\lambda^3}{L_\parallel}. \quad (149)$$

Expressing the energy flux in terms of the total turbulent energy, we obtain the dissipation scale in the form

$$\lambda = \left(\frac{6\eta^2 L_\perp}{\gamma_A^2 W} \right)^{1/3}. \quad (150)$$

4.3 Ampère force

The last two terms in Euler equation (50) are related to the displacement current. The calculation of the force per unit mass yields (see Appendix A)

$$\begin{aligned} \mathbf{f}_D &= -\frac{1}{4\pi\rho} \left\langle \frac{1}{c} \frac{\partial \delta^{(1)} \mathbf{E}}{\partial t} \times \delta \mathbf{B} \right\rangle - \frac{1}{4\pi\rho} \left\langle \frac{1}{c} \frac{\partial \delta^{(2)} \mathbf{E}}{\partial t} \right\rangle \times \mathbf{B} \\ &= \left\{ \left(\frac{\hat{\mathbf{T}}}{2} - \hat{\mathbf{I}} \right) \left[\frac{\partial \mathbf{v}}{\partial t} - \left(\nabla \mathbf{v} + \frac{\eta}{3L_\parallel^2} + \frac{\eta}{L_\perp \lambda} \right) \mathbf{v} \right] \right. \\ &\quad \left. + \frac{1}{2} \gamma_A^2 \mathbf{a} \times \text{rot } \mathbf{a} \right\} \frac{W}{c^2} + \left[\left(\hat{\mathbf{T}} \frac{\partial \mathbf{a}}{\partial t} \right) \times \text{rot } \mathbf{a} \right] \frac{\eta_w}{2c^2}. \quad (151) \end{aligned}$$

We estimate the plasma velocity as $v \sim L_\perp/T$, the gradient operator as $\nabla \sim 1/L_\perp$, and the turbulent magnetic viscosity as $\eta_w \sim \gamma_A^2 W \tau$. The terms in formula (151) then compare as

$$1 : 1 : \frac{L_\perp}{L_\parallel} \frac{\eta}{L_\parallel v} : \left(\frac{\eta}{L_\perp v} \frac{W}{v^2} \right)^{1/3} : \frac{\gamma_A^2 a^2 W}{v^2 c^2} : \frac{\gamma_A^2 a^2 \tau W}{v L_\perp c^2}. \quad (152)$$

Clearly, in the case of a high Alfvén velocity, the last two terms dominate. Then, if the Alfvén relaxation regime is realized, i.e., $\tau = \tau_A \sim L_\parallel/(\gamma_A a)$, the last two terms compare as

$$\frac{\gamma_A a}{v} : \frac{L_\parallel}{L_\perp}. \quad (153)$$

It is easy to see that if $v \ll c$, the last term is small, and the expression for the force takes the form

$$\mathbf{f}_D = \frac{\gamma_A^2 W}{2c^2} \frac{\mathbf{B} \times \text{rot } \mathbf{B}}{4\pi\rho}. \quad (154)$$

If the diffusion relaxation regime is realized, $\tau = \tau_d \sim L_\perp^2/\eta$, the last two terms compare as

$$\eta : L_\perp v. \quad (155)$$

At the same time, in the diffusion regime, the inequality $L_\parallel/L_\perp > \gamma_A a L_\perp/\eta$ holds [see (130)]. Because $\gamma_A a/v \gg L_\parallel/L_\perp$, formula (154) for the force \mathbf{f}_D is also valid in the diffusion regime.

4.4 Turbulent heating

Turbulent heating is already nonzero in the first order of the expansion in the relaxation time:

$$\langle (\text{rot } \delta \mathbf{b})^2 \rangle^{(0)} = \sum_{\pm} \int d^3 k k_\perp^2 P_{\pm}. \quad (156)$$

Because the transverse part of the power density is proportional to k_\perp^{-2} , this integral diverges in the limit $k_\perp \rightarrow \infty$. To avoid the divergence, it is necessary to rigorously take into account the finite upper integration limit over transverse wave numbers, which is equal to the inverse dissipation scale λ^{-1} . As a result, we obtain (by ignoring L_\perp^{-1} compared to λ^{-1})

$$\langle (\text{rot } \delta \mathbf{b})^2 \rangle = \frac{W}{L_\perp \lambda} = 0.55 \frac{\gamma_A^{1/3} W^{4/3}}{\eta^{2/3} L_\perp^{4/3}}. \quad (157)$$

In this equality, we used dissipation scale (150).

In entropy equation (52), the term responsible for the turbulent heating has the form

$$\left(\frac{\partial s}{\partial t} \right)_w = \frac{q_w}{T}, \quad (158)$$

where q_w determines the rate of change of the specific internal gas energy with an adiabatic exponent γ . At constant density, it turns out to be

$$q_w = \eta \langle (\text{rot } \delta \mathbf{b})^2 \rangle = 0.55 \frac{\eta^{1/3} W^{4/3}}{L_\perp^{4/3}}. \quad (159)$$

Equation (52) also contains the heat sources due to the displacement current dissipation (see Appendix B):

$$\begin{aligned} \frac{q_D}{\eta} &= \frac{(\gamma_A \mathbf{a} \times \mathbf{v})^2}{2c^4} \frac{W}{L_\perp \lambda} \\ &+ \left\{ 2 + \left[\frac{\gamma_A^2 a^2}{c^2} + \left(1 - \frac{\gamma_A^2 a^2}{2c^2} \right) \frac{v_\parallel^2}{c^2} \right] \right\} \frac{\gamma_A^2 a^2}{c^2} \frac{W}{3L_\parallel^2} \\ &+ [(\hat{\mathbf{T}} \text{rot } \mathbf{a}) \times \text{rot } \mathbf{a}] \frac{\gamma_A^2 W}{c^2} - [\hat{\mathbf{T}}(\gamma_A \mathbf{a} \times \text{rot } \mathbf{a})]^2 \frac{\gamma_A^2 W}{2c^4}. \quad (160) \end{aligned}$$

The terms in the right-hand side of this formula compare as

$$\frac{v^2}{c^2} \frac{L_\parallel^2}{L_\perp \lambda} : 1 : \frac{\gamma_A^2 a^2}{c^2} : \frac{v^2}{c^2} : \frac{\gamma_A^2 a^2}{c^2} \frac{v^2}{c^2} : \frac{L_\parallel^2}{L_\perp^2} : \frac{\gamma_A^2 a^2}{c^2} \frac{L_\parallel^2}{L_\perp}. \quad (161)$$

In expression (160), the first and the next-to-last terms dominate. Their ratio is

$$\frac{v^2}{c^2} : \frac{\lambda}{L_\perp}. \quad (162)$$

The dissipation scale λ is defined according to (150). Using (157) and (159), we can write

$$\frac{q_D}{\eta} = \left[\frac{(\mathbf{a} \times \mathbf{v})^2}{2c^4} + \frac{(\hat{\mathbf{T}} \text{rot } \mathbf{a}) \times \text{rot } \mathbf{a}}{c^2} L_\perp \lambda \right] \gamma_A^2 \frac{q_w}{\eta}. \quad (163)$$

Because $v \ll c$ and $\lambda \ll L_\perp$, as well as $\gamma_A a/c < 1$, it is clear that $q_D \ll q_w$. Thus, the displacement current does not contribute to the turbulent plasma heating.

5. Analysis

5.1 Summary of the results

In Section 4, we computed sources of turbulent pressure, viscosity, and heating. They were expressed through double correlators of the Alfvén velocity and magnetic field perturbations. The values of the double correlators were calculated in the first nonvanishing order of the τ -approximation. The power density of Alfvén wave turbulence was taken from [24]. For simplicity, only the isotropic contribution (in the transverse wave numbers) of the double correlators to the sources was taken into account.

We write the full system of MHD equations with turbulent sources in the final form:

$$\frac{\partial \rho}{\partial t} + \nabla(\rho \mathbf{v}) = 0, \quad (164)$$

$$\begin{aligned} \frac{\partial \mathbf{v}}{\partial t} + (\mathbf{v} \nabla) \mathbf{v} = & -\frac{1}{\rho} \nabla \left[P + \left(\hat{\mathbf{I}} - \frac{\gamma_A^2 a^2}{c^2} \hat{\mathbf{T}} \right) \frac{\rho W}{2} \right] \\ & - \left(1 + \frac{\gamma_A^2 W}{2c^2} \right) \frac{\mathbf{B} \times \text{rot } \mathbf{B}}{4\pi\rho}, \end{aligned} \quad (165)$$

$$\frac{\partial \mathbf{B}}{\partial t} - \text{rot} [\mathbf{v} \times \mathbf{B} - (\eta + \eta_w \hat{\mathbf{T}}) \text{rot } \mathbf{B}] = 0, \quad (166)$$

$$\frac{\partial s}{\partial t} + (\mathbf{v} \nabla) s = \frac{\eta}{T} \frac{(\text{rot } \mathbf{B})^2}{4\pi\rho} + \frac{q_w}{T}. \quad (167)$$

In Euler equation (165), wave turbulence appears via the anisotropic stress tensor and the relativistic correction to the Ampère force. The anisotropic character is defined by the projection tensor

$$\hat{\mathbf{T}} = \hat{\mathbf{I}} - \mathbf{e}_\parallel \otimes \mathbf{e}_\parallel, \quad (168)$$

where \mathbf{e}_\parallel is the unit vector along the local field \mathbf{B} .

The turbulent energy per unit mass W includes the energy of the ensemble of Alfvén waves with the corresponding power spectrum (112)

$$W = 2.34 \sqrt{\epsilon a} \frac{L_\perp}{L_\parallel}, \quad (169)$$

where ϵ is the energy flux through the inertial interval, $a = B/\sqrt{4\pi\rho}$ is the Alfvén velocity, and L_\parallel and L_\perp are the longitudinal and transverse turbulence scales.

In the magnetic induction equation, the wave turbulence appears as the transverse magnetic viscosity tensor. The turbulent viscosity coefficient is

$$\eta_w = \frac{\gamma_A^2}{2\eta} W L_\parallel^2 \hat{\alpha}^2 \left[\frac{1}{3} + \frac{\alpha^2}{\hat{\alpha}^2} \left(\ln \frac{\beta^2}{\hat{\alpha}^2} + \frac{4}{3} \frac{\alpha}{\beta} - \frac{4}{3} \frac{\alpha}{\hat{\alpha}} \right) \right], \quad (170)$$

where $\hat{\alpha} = \min(\alpha, \beta)$, $\alpha = [2\eta/(\gamma_A a L_\parallel)]^{1/2}$, and $\beta = L_\perp/L_\parallel$.

In the entropy equation, only one term,

$$q_w = \eta \frac{W}{L_\perp \lambda}, \quad (171)$$

is due to turbulence, with the dissipation scale λ given by

$$\lambda = \left(\frac{6\eta^2 L_\perp}{\gamma_A^2 W} \right)^{1/3}. \quad (172)$$

To complete the system of MHD equations (164)–(167), it is necessary to define the longitudinal L_\parallel and transverse L_\perp scales, as well as the turbulent energy W or the energy flux ϵ . The last two quantities determine the intensity of turbulent velocity and magnetic field pulsations. In model (164)–(167), it is essential that the background magnetic field and turbulent intensity are independent variables. Depending on the relation between them, the proposed model can describe significantly different physical situations.

We first consider the weak-field limit, or, more precisely, the approximation in which the Alfvén velocity is low, $a \ll c$. In this approximation, the anisotropic part of turbulent pressure in equation of motion (165) vanishes. If the turbulent energy also tends to zero, then, clearly, the model reduces to the usual MHD case. Otherwise, depending on the value of turbulent energy, turbulence can appear on the dynamical time scale (pressure and the Ampère force) or dissipative time scale (viscosity and heating). We note that the turbulent viscosity coefficient in this approximation is determined by the Ohmic diffusion time (see Section 4.2) and has form (146).

In the opposite limit, when the turbulent energy is small but nonzero and the Alfvén velocity is comparable to the speed of light, the anisotropic part of turbulent pressure and the relativistic correction to the Ampère force become significant. The diffusion coefficient η_w is now determined by the Alfvén time and decreases as Alfvén velocity (147) increases. Because the heat source q_w in entropy equation (167) depends on the turbulent energy to the power 4/3, its role in thermal balance can be small.

In the limit of extremely high Alfvén velocities, $a \gg c$, the proposed model is inapplicable in general because we have used approximate relations for relativistic Alfvén waves (72) and (73). However, in this case, model (164)–(167) does not lead to unphysical consequences either. Indeed, at high Alfvén velocities, the factor γ_A tends to zero. Consequently, all turbulent terms except the isotropic part of turbulent pressure disappear from the equations. In the limit $a \gg c$, Alfvén waves degenerate into magnetic field oscillations (see Section 3.1) and therefore the turbulent pressure should be regarded as the radiation pressure.

5.2 Estimates

As a possible astrophysical application, in Section 2.1 we mentioned the problem of gas accretion in polars and intermediate polars. Below, we consider two examples of such systems: AM Herculis and ER Hydrae, and estimate the effect of turbulent sources on the accretion process.

For the binary system with the polar-like AM Herculis, we adopt the respective accretor and donor masses $M_1 = 0.5 M_\odot$ and $M_2 = 0.25 M_\odot$, the accretor radius $R_1 = 1.3 \times 10^{-2} R_\odot$, the binary orbital period $P_{\text{orb}} = 3.1$ h, and the mass accretion rate onto the white dwarf $\dot{M} = 10^{-8} M_\odot \text{ yr}^{-1}$. The gas temperature T is fixed at 10^4 K. We assume the white dwarf in this system to have a strong dipole magnetic field $B_1 \sim 10^7$ G on the surface. Numerical simulations of such systems in [27, 28] have suggested that such a strong field almost completely controls the gas flow inside the Roche lobe of the white dwarf. The accretion flow forms a column stream

that starts at the Lagrange point L_1 , goes to the magnetospheric boundary, and then flows into the polar region of the white dwarf along the magnetic field lines.

The magnetospheric radius R_m can be estimated as the Alfvén radius from the relation

$$\frac{B}{\sqrt{4\pi\rho}} = v_{\text{ff}}, \quad (173)$$

where $v_{\text{ff}} = (2GM_1/R_m)^{1/2}$ is the free-fall velocity. Using the mass conservation law in the form $\dot{M} = \rho v_{\text{ff}} 4\pi R_m^2$, we obtain

$$R_m = \left(\frac{B_1^4 R_1^{12}}{2GM_1 \dot{M}^2} \right)^{1/7}. \quad (174)$$

In the system under consideration, $R_m = 3.4 \times 10^{10}$ cm, which is about half the distance between the binary system components. The cross section of the accretion stream in the system with a polar can be assumed to be equal to the stream cross section at the Lagrange point L_1 [13, (2.10)]:

$$S_{\text{str}} = \frac{\pi c_s^2}{4\Omega_{\text{orb}}^2}, \quad (175)$$

where c_s is the speed of sound and $\Omega_{\text{orb}} = 2\pi/P_{\text{orb}}$ is the angular orbital velocity of the binary system.

We estimate the effect of different terms in Eqns (164)–(167): the characteristic dynamical time

$$\tau_{\text{dyn}} = \frac{L_{\parallel}^{3/2}}{\sqrt{GM_1}}, \quad (176)$$

the electromagnetic induction time

$$\tau_{\text{ind}} = \frac{L_{\perp}}{v_{\text{ff}}}, \quad (177)$$

$$\tau_A = \frac{L_{\parallel}}{a}, \quad (178)$$

the time of establishing the turbulent cascade (mentioned in Section 2.1 as the energy redistribution time in the cascade)

$$\tau_{\text{casc}} = \frac{L_{\perp}^2 a}{L_{\parallel} W}, \quad (179)$$

the characteristic time of turbulent viscosity

$$\tau_{\text{visc}} = \frac{L_{\perp}^2}{\eta_w}, \quad (180)$$

the turbulent heating time

$$\tau_{\text{heat}} = \frac{k_B T}{m_p q_w}, \quad (181)$$

the magnetic Reynolds number

$$R_m = \frac{L_{\perp} v_{\text{ff}}}{\eta}, \quad (182)$$

and the turbulent magnetic Reynolds number

$$R_w = \frac{L_{\perp} v_{\text{ff}}}{\eta_w}. \quad (183)$$

To calculate the times τ_{visc} and τ_{heat} , as well as the Reynolds number R_m , it is necessary to know the Ohmic magnetic viscosity $\eta = c^2/(4\pi\sigma)$, where the electric conductivity is

$$\sigma = \frac{e^2 n \tau}{m_e}. \quad (184)$$

Here, τ is the characteristic time of electron–ion collisions [42],

$$\tau = \frac{T^{3/2}}{5.5nA_C}, \quad (185)$$

where $A_C = \ln(220Tn^{-1/3})$ is the Coulomb logarithm.

The times τ_{casc} , τ_{visc} , and τ_{heat} are also determined by the longitudinal and transverse scales of turbulence and by turbulent energy. We set the longitudinal scale equal to the magnetosphere radius, $L_{\parallel} = R_m$, and define the transverse scale as the accretion stream size, $L_{\perp} = S_{\text{str}}^{1/2}$. To estimate the turbulent energy, we ascribe the turbulence a certain ‘effective’ temperature T_w ,

$$W = \frac{3k_B T_w}{m_p}. \quad (186)$$

We consider two limit cases: (a) the turbulent energy is equal to the thermal energy of the medium with a temperature of the order of 10^4 K; (b) the value of the energy is determined by the matter temperature at the accretion column base, which is about 10^8 K [10]. We refer to these cases as the respective weak and strong turbulence.

Finally, we take the gas number density in the accretion column $n = 10^{15}$ cm $^{-3}$ and assume its temperature to be $T = 10^4$ K. The resulting estimates are listed in Table 2. It is seen that in the case of weak turbulence, the formation time of

Table 2. Characteristics* of the accretion flow for systems like AM Herculis (the first pair of columns) and EX Hydrae (the second pair of columns). The first and second columns in the pair respectively correspond to the weak and strong turbulence.

	AM Herculis		EX Hydrae	
	$T_w = 10^4$ K	$T_w = 10^8$ K	$T_w = 10^4$ K	$T_w = 10^8$ K
B_1 , G	10 ⁷		10 ⁴	
B , G	1.8 × 10 ²		5.1 × 10 ²	
n , cm ⁻³	10 ¹⁵		10 ¹⁵	
L_{\parallel} , cm	3.4 × 10 ¹⁰		2.4 × 10 ⁹	
L_{\perp} , cm	1.4 × 10 ⁹		1.3 × 10 ⁷	
τ_{dyn}^{-1} , s ⁻¹	1.8 × 10 ⁻³		1.0 × 10 ⁻¹	
τ_{ind}^{-1} , s ⁻¹	4.3 × 10 ⁻²		19.0	
τ_A^{-1} , s ⁻¹	3.6 × 10 ⁻⁵		1.4 × 10 ⁻³	
η , cm ² s ⁻¹	4.8 × 10 ⁶		4.8 × 10 ⁶	
η_w , cm ² s ⁻¹	5.7 × 10 ¹⁷	5.7 × 10 ²¹	9.6 × 10 ¹⁵	9.6 × 10 ¹⁹
τ_{casc}^{-1} , s ⁻¹	3.3 × 10 ⁻²	3.3 × 10 ²	10.5	1.1 × 10 ⁵
τ_{visc}^{-1} , s ⁻¹	2.8 × 10 ⁻¹	2.8 × 10 ³	58.3	5.8 × 10 ⁵
τ_{heat}^{-1} , s ⁻¹	1.6 × 10 ⁻⁶	3.3 × 10 ⁻¹	8.3 × 10 ⁻⁴	1.8 × 10 ²
R_m	1.9 × 10 ¹⁰		6.6 × 10 ⁸	
R_w	1.5 × 10 ⁻¹	1.5 × 10 ⁻⁵	3.3 × 10 ⁻¹	3.3 × 10 ⁻⁵

* B_1 and B are the respective magnetic fields on the accretor surface and at the magnetosphere boundary; n is the particle number density; L_{\parallel} and L_{\perp} are the longitudinal and transverse turbulence scale; η is the Ohmic viscosity coefficient; η_w is the magnetic turbulent viscosity coefficient; R_m and R_w are the respective Ohmic and turbulent magnetic Reynolds numbers; τ_{\dots}^{-1} are the inverse times.

the turbulent cascade is comparable to the magnetic induction time and almost one order of magnitude shorter than the dynamical time, and the turbulent viscosity dominates over other effects. The turbulent heating must then be small. When $T_w = 10^8$ K, all turbulence-related effects increase by four to five orders of magnitude and should dominate over the ideal MHD effects. In particular, the turbulent magnetic Reynolds number is smaller than the Ohmic Reynolds number by 9–15 orders of magnitude.

Similar estimates can be obtained for the system with an intermediate polar like EX Hydrae. The respective accretor and donor masses are $M_1 = 0.79 M_\odot$ and $M_2 = 0.096 M_\odot$, the accretor radius is $R_1 = 1.3 \times 10^{-2} R_\odot$, the accretion rate is $\dot{M} = 10^{-10} M_\odot \text{ yr}^{-1}$, the binary orbital period is $P_{\text{orb}} = 1.64$ h, and the white dwarf magnetic field is $B_1 = 10^4$ G. In such systems, the magnetosphere radius is relatively small. Leaving the inner Lagrange point, the stream forms a disk, and reaching the magnetosphere, the stream falls onto the white dwarf by forming an accretion column (or accretion curtain, better to say) [28]. We again assume the longitudinal turbulence scale to be equal to the Alfvén radius and the transverse scale to be equal to the isothermal disk thickness at the Alfvén radius, $L_\perp = L_\parallel c_s / v_K$, where v_K is the Keplerian rotation velocity. Estimates for such a system are also given in Table 2. As in the case with a polar, the turbulence significantly exceeds the effects from ordinary MHD terms in Eqns (164)–(167).

5.3 Strong turbulence approximation

The modified MHD model used in our previous papers [27, 28] corresponds to the strong turbulence limit in plasma flows in a strong external magnetic field. We show how to pass to this model from Eqns (164)–(167). The total magnetic field \mathbf{B} in such a plasma can be represented as the sum of the external magnetic field \mathbf{H} and the magnetic field \mathbf{b} induced by electric currents in the plasma, $\mathbf{B} = \mathbf{H} + \mathbf{b}$. Because the background magnetic field \mathbf{H} is produced by external sources outside the spatial domain of interest, it must satisfy the potentiality condition $\text{rot } \mathbf{H} = 0$. Induction equation (166) can be rewritten in the form

$$\frac{\partial \mathbf{b}}{\partial t} + \frac{\partial \mathbf{H}}{\partial t} - \text{rot}(\mathbf{v} \times \mathbf{b} + \mathbf{v} \times \mathbf{H} - \eta_w \text{rot}_\perp \mathbf{b}) = 0. \quad (187)$$

Here, we disregarded the Ohmic diffusion compared to the turbulent one ($\eta \ll \eta_w$). The index \perp denotes components transverse to the magnetic field vector.

The simplest case corresponds to a stationary magnetic field, $\partial \mathbf{H} / \partial t = 0$. However, problems are frequently encountered when the magnetic field is nonstationary. This is the case, for example, in modeling plasma flow around a rotating magnetized star with the magnetic axis misaligned with the spin axis. In principle, the external magnetic field can change in time due to variability of its sources. For example, this can be due to a variable stellar magnetic moment. However, these changes typically occur on long time scales [6] and are ignored in what follows. Therefore, the equation for the external magnetic field can be written as (see, e.g., [1])

$$\frac{\partial \mathbf{H}}{\partial t} = \text{rot}(\mathbf{V} \times \mathbf{H}). \quad (188)$$

Here, the right-hand side is due to the effect of motion of the source as a whole, and the vector \mathbf{V} determines the velocity of the source at a given point. It is equal to the velocity of the

external magnetic field lines in a vacuum (i.e., without plasma). For example, if the field change is caused by rotation of a star (the stellar center is at the coordinate origin) with an angular velocity $\boldsymbol{\Omega}$, then the velocity is $\mathbf{V} = \boldsymbol{\Omega} \times \mathbf{r}$.

We consider the case of a strong external magnetic field $H \gg b$ under strong turbulence conditions, when the magnetic Reynolds number R_m caused by wave turbulence is small, $R_w \ll 1$ [43]. As shown above (see the preceding section), this situation can occur in the magnetospheres of white dwarfs in polars and intermediate polars. Retaining the leading terms in Eqn (187), we find

$$\text{rot}[(\mathbf{v} - \mathbf{V}) \times \mathbf{H} - \eta_w \text{rot}_\perp \mathbf{b}] = 0. \quad (189)$$

This, in particular, implies that the induced field is by an order of magnitude equal to $b \approx R_w H$, and in the limit of small magnetic Reynolds numbers $R_w \ll 1$, it is indeed small compared to the background field, $b \ll H$.

The quantity under the curl operator in the left-hand side of (189) is equal to $-c\mathbf{E}$, where \mathbf{E} is the electric field in the plasma. Equation (189) implies that this field is potential, $\mathbf{E} = -\nabla\varphi$, where φ is the corresponding scalar potential. Therefore, we can write

$$(\mathbf{v} - \mathbf{V}) \times \mathbf{H} - \eta_w \text{rot}_\perp \mathbf{b} = c \nabla\varphi. \quad (190)$$

This equation defines the component of the potential gradient that is transverse to the magnetic field. To find the potential itself, we extend Eqn (190) by changing $\text{rot}_\perp \mathbf{b}$ to $\text{rot } \mathbf{b}$ and calculate the divergence of the left- and right-hand sides. Assuming for simplicity that the viscosity coefficient is constant, we then obtain

$$\nabla^2 \phi = \frac{1}{c} \mathbf{H} \text{rot}(\mathbf{v} - \mathbf{V}). \quad (191)$$

In calculating the right-hand side of this equation, we used the potentiality condition $\text{rot } \mathbf{H} = 0$ for the magnetic field.

The electromagnetic force in equation of motion (165) is

$$\mathbf{f}_{\text{em}} = -\chi_D \frac{\mathbf{B} \times \text{rot } \mathbf{B}}{4\pi\rho} = -\chi_D \frac{\mathbf{b} \times \text{rot } \mathbf{b}}{4\pi\rho} - \chi_D \frac{\mathbf{H} \times \text{rot } \mathbf{b}}{4\pi\rho}, \quad (192)$$

where $\chi_D = 1 + \gamma_A^2 W / (2c^2)$ is the coefficient due to the displacement current. The second term in the right-hand side describes the force

$$\mathbf{f}_{\text{em}}^{(2)} = -\chi_D \frac{\mathbf{H} \times \text{rot } \mathbf{b}}{4\pi\rho} \quad (193)$$

acting in the plasma due to the external magnetic field. This force can be computed in the approximation considered above. By expressing $\text{rot } \mathbf{b}$ from (190) and substituting it in (193), we find

$$\mathbf{f}_{\text{em}}^{(2)} = -\frac{\chi_D H^2}{4\pi\rho\eta_w} (\mathbf{v} - \mathbf{V})_\perp + \frac{\chi_D c}{4\pi\rho} \mathbf{H} \times \nabla\varphi. \quad (194)$$

It is convenient to introduce the local velocity of magnetic field lines \mathbf{u} (the magnetic field line velocity in the comoving frame where $\partial \mathbf{H} / \partial t = 0$) from the condition

$$\mathbf{E} = -\nabla\varphi = -\frac{1}{c} \mathbf{u} \times \mathbf{H}. \quad (195)$$

From this formula, we can obtain

$$\mathbf{u}_\perp = \frac{c}{H^2} (\mathbf{E} \times \mathbf{H}) = \frac{c}{H^2} (\mathbf{H} \times \nabla\varphi). \quad (196)$$

The expression for electromagnetic force (194) can then be finally rewritten in the form

$$\mathbf{f}_{\text{em}}^{(2)} = -\frac{(\mathbf{v} - \mathbf{U})_\perp}{t_w}, \quad (197)$$

where the total velocity of the magnetic field lines is $\mathbf{U} = \mathbf{V} + \mathbf{u}$, and the relaxation time is

$$t_w = \frac{4\pi\rho\eta_w}{\chi_D H^2}. \quad (198)$$

An interesting interpretation of electromagnetic force (197) can be suggested in terms of a friction force. Indeed, it is well known (see, e.g., [2]) that in a plasma containing several particle species, the specific friction force between components α and β is

$$\mathbf{f}_{\alpha\beta} = -v_{\alpha\beta}(\mathbf{v}_\alpha - \mathbf{v}_\beta), \quad (199)$$

where \mathbf{v}_α and \mathbf{v}_β are velocities of the corresponding plasma components, and $v_{\alpha\beta}$ is the characteristic collision rate of species α and β . A comparison of this expression with (197) suggests that (197) represents a friction force between the plasma and magnetic field lines. Here, the corresponding collision rate is $v_w = t_w^{-1}$. The appearance of a finite collision rate can be related to the fact that magnetic field lines chaotically oscillate in a turbulent plasma, which results in some effective ‘collision cross section’ for plasma particles with the magnetic field. Thus, in a turbulent plasma, a strong external magnetic field plays the role of an additional ‘effective’ fluid with which the plasma interacts due to the friction force. We stress that this effect occurs only in the direction perpendicular to the magnetic field. In the longitudinal direction, plasma flows freely.

When using the approximation under study, the initial equations (164)–(167) can be significantly simplified. If, in addition, we can ignore the turbulent pressure and heating, they reduce to the system of equations

$$\frac{\partial\rho}{\partial t} + \nabla(\rho\mathbf{v}) = 0, \quad (200)$$

$$\frac{\partial\mathbf{v}}{\partial t} + (\mathbf{v}\nabla)\mathbf{v} = -\frac{\nabla P}{\rho} - \frac{\mathbf{b} \times \text{rot } \mathbf{b}}{4\pi\rho} - \frac{(\mathbf{v} - \mathbf{U})_\perp}{t_w}, \quad (201)$$

$$\frac{\partial\mathbf{b}}{\partial t} = \text{rot} [\mathbf{v} \times \mathbf{b} + (\mathbf{v} - \mathbf{V}) \times \mathbf{H} - \eta_w \text{rot}_\perp \mathbf{b}], \quad (202)$$

$$\frac{\partial s}{\partial t} + (\mathbf{v}\nabla)s = 0. \quad (203)$$

It is exactly this model that we have used in our previous studies [13, 27, 28]. Here, to be fair, we should say that to simplify calculations, we have disregarded the velocity \mathbf{u} and assumed that $\mathbf{U} = \mathbf{V}$. It is important to note that if there is no external magnetic field, $\mathbf{B} = \mathbf{b}$, and no wave turbulence, this system reduces to the ideal MHD equations. In the opposite limit of a strong external magnetic field $H \gg b$ and strong turbulence $R_w \ll 1$, induction equation (202) reduces to (189), and the second term in the right-hand side of (201) can be ignored. As a result, we arrive at hydrodynamic equations with additional force (197). In the intermediate cases, system

of equations (200)–(203) does not accurately describe the flow structure. For a more precise treatment, the full system of equations (164)–(167) should be used.

6. Conclusion

We have studied the problem of modeling astrophysical plasma flows in strong magnetic fields. Under these conditions, the classical MHD approximation can be incorrect, and therefore alternative approaches should be sought to describe such flows. One of the possibilities is to account for wave (Alfvén) turbulence that can develop in such systems. Indeed, in the plasma in a strong magnetic field, over the characteristic dynamic time, Alfvén and magnetosonic waves can travel many times across the flow in the longitudinal and transverse directions with respect to the external magnetic field. The interaction of these waves redistributes energy between different harmonics, thus forming a turbulent cascade. Wave turbulence, in particular, is observed in the solar wind plasma and in Earth’s polar wind [37]. To describe such flows, it is possible to use the standard ensemble averaging over wave pulsations.

We have considered this approach in application to astrophysical flows. We plan to apply this model in the future to describe plasma flows in strong external magnetic fields; therefore, in the basic equations, we included relativistic effects related to high propagation velocities of Alfvén and magnetosonic waves. A turbulent flow is treated as the sum of the mean flow and perturbations caused by wave pulsations. In this approach, it is possible to obtain a complete system of equations for the mean flow characteristics. In the equations for mean characteristics, the source terms caused by wave pressure, turbulent magnetic viscosity, and turbulent wave heating are taken into account. All transport coefficients are computed using the wave turbulence spectrum calculated in [24].

The modified MHD equations (164)–(167) derived here can be used to model a wide class of astrophysical plasma flows. It is shown that for plasma flows in strong external fields and with strong turbulence, these equations take a simpler form (200)–(203), which corresponds to a semi-phenomenological model we used in our previous studies [27, 28]. Thus, this model acquired a more rigorous justification.

We note several important points. In this paper, we started from semirelativistic MHD equations. However, to calculate double correlators, we used the wave turbulence spectrum obtained in the nonrelativistic MHD approach. In our model, this factor is not essential. First, only the power-law character of the turbulence spectrum in the inertial interval is important in our model, and the turbulent energy and the power-law exponent are free model parameters. Second, in the final equations, all information on the turbulence spectrum is encoded in the transport coefficients, which are not known precisely anyway.

As pointed out in Section 3.3, an important assumption made in calculating the turbulence spectrum was that the spectrum is balanced. In this case, the energy of waves propagating along the field in one direction is equal to that propagating in the opposite direction. Clearly, this condition can be violated in the general case. For example, it is known that in the solar wind, the energy of waves propagating against the field is about one tenth of the energy of waves propagating along the field. However, if the spectrum here

remains a power-law one (as is the case in the solar wind), all conclusions remain valid after changing the corresponding parameters.

Thus, the modified MHD model proposed in this paper is universal and can be applied to a wide range of astrophysical flows.

The authors thank S N Zamozdra for the useful discussions during the preparation of this paper. The work of E P Kurbatov is supported by the Russian Foundation for Basic Research (project 14-29-06059). The work of A G Zhilkin is supported by the Russian Science Foundation (project 15-12-30038).

Appendix. Turbulent sources related to the displacement current

A. Equations of motion

Here, we provide calculations of turbulent sources for Euler equation (50) related to the displacement current. We write the expression for the force keeping only the terms quadratic in perturbations:

$$\begin{aligned} \mathbf{f}_D &= -\frac{1}{4\pi\rho} \left\langle \frac{1}{c} \frac{\partial \delta^{(1)} \mathbf{E}}{\partial t} \times \delta \mathbf{B} \right\rangle - \frac{1}{4\pi\rho} \left\langle \frac{1}{c} \frac{\partial \delta^{(2)} \mathbf{E}}{\partial t} \right\rangle \times \mathbf{B} \\ &= \frac{1}{c^2} \left(\mathbf{a} \left\langle \frac{\partial \delta \mathbf{v}}{\partial t} \delta \mathbf{b} \right\rangle + \frac{\partial \mathbf{v}}{\partial t} \langle \delta \mathbf{b} \otimes \delta \mathbf{b} \rangle - \frac{\partial \mathbf{v}}{\partial t} \langle |\delta \mathbf{b}|^2 \rangle \right) \\ &\quad + \mathbf{v} \left\langle \delta \mathbf{b} \otimes \frac{\partial \delta \mathbf{b}}{\partial t} \right\rangle - \mathbf{v} \left\langle \delta \mathbf{b} \frac{\partial \delta \mathbf{b}}{\partial t} \right\rangle + \frac{\partial \mathbf{a}}{\partial t} \langle \delta \mathbf{v} \delta \mathbf{b} \rangle \\ &\quad - \frac{\partial \mathbf{a}}{\partial t} \langle \delta \mathbf{b} \otimes \delta \mathbf{v} \rangle + \mathbf{a} \left\langle \frac{\partial \delta \mathbf{v}}{\partial t} \otimes \delta \mathbf{b} \right\rangle - \mathbf{a} \left\langle \frac{\partial \delta \mathbf{b}}{\partial t} \otimes \delta \mathbf{v} \right\rangle. \end{aligned} \quad (204)$$

(1) In the first term in the right-hand side of (204), the only potentially nonzero term that arises in the first order of the τ -approximation contains the square of the polarization vector and hence vanishes:

$$\begin{aligned} \mathbf{a} \left\langle \frac{\partial \delta \mathbf{v}}{\partial t} \delta \mathbf{b} \right\rangle^{(1)} &= \gamma_A^2 \mathbf{a} \sum_{\pm} \int d^3 k \langle (\text{rot } \mathbf{a} \times \delta \tilde{\mathbf{b}}) \delta \tilde{\mathbf{b}} \rangle_{\pm} \\ &= \gamma_A^2 \mathbf{a} \sum_{\pm} \int d^3 k [(\mathbf{e}_n \times \mathbf{e}_n) \text{rot } \mathbf{a}] P_{\pm} = 0. \end{aligned} \quad (205)$$

(2) The second term is already nonzero in the zeroth order of the τ -approximation:

$$\frac{\partial \mathbf{v}}{\partial t} \langle \delta \mathbf{b} \otimes \delta \mathbf{b} \rangle^{(0)} = \hat{\mathbf{T}} \frac{\partial \mathbf{v}}{\partial t} \frac{W}{2}. \quad (206)$$

(3) The third term is computed similarly to the second term:

$$-\frac{\partial \mathbf{v}}{\partial t} \langle |\delta \mathbf{b}|^2 \rangle^{(0)} = -\frac{\partial \mathbf{v}}{\partial t} W. \quad (207)$$

(4) The fourth term is represented by two nonvanishing terms:

$$\mathbf{v} \left\langle \delta \mathbf{b} \otimes \frac{\partial \delta \mathbf{b}}{\partial t} \right\rangle^{(1)} = -\mathbf{v} \sum_{\pm} \int d^3 k (\nabla \mathbf{v} + \eta k^2) \langle \delta \tilde{\mathbf{b}} \otimes \delta \tilde{\mathbf{b}} \rangle_{\pm}. \quad (208)$$

The first term here can be computed in the same way as (206). The integral for the second term can be easily found using (157); here, the contribution due to longitudinal wave numbers in the integrand can be ignored:

$$\begin{aligned} \sum_{\pm} \int d^3 k k^2 \langle \delta \tilde{\mathbf{b}} \otimes \delta \tilde{\mathbf{b}} \rangle_{\pm} &= \hat{\mathbf{T}} \sum_{\pm} \int d^3 k (k_{\parallel}^2 + k_{\perp}^2) P_{\pm} \\ &= \hat{\mathbf{T}} \left(\frac{W}{3L_{\parallel}^2} + \frac{W}{L_{\perp} \lambda} \right). \end{aligned} \quad (209)$$

As a result, we have

$$\mathbf{v} \left\langle \delta \mathbf{b} \otimes \frac{\partial \delta \mathbf{b}}{\partial t} \right\rangle^{(1)} = -\hat{\mathbf{T}} \mathbf{v} \left(\nabla \mathbf{v} + \frac{\eta}{3L_{\parallel}^2} + \frac{\eta}{L_{\perp} \lambda} \right) \frac{W}{2}. \quad (210)$$

(5) The fifth term is calculated similarly to the fourth one, but has an isotropic form:

$$-\mathbf{v} \left\langle \delta \mathbf{b} \frac{\partial \delta \mathbf{b}}{\partial t} \right\rangle^{(1)} = \mathbf{v} \left(\nabla \mathbf{v} + \frac{\eta}{3L_{\parallel}^2} + \frac{\eta}{L_{\perp} \lambda} \right) W. \quad (211)$$

(6) The sixth term is processed using (84) and vanishes similarly to (205):

$$\frac{\partial \mathbf{a}}{\partial t} \langle \delta \mathbf{v} \delta \mathbf{b} \rangle^{(1)} = \gamma_A^2 \frac{\partial \mathbf{a}}{\partial t} \sum_{\pm} \int d^3 k [(\mathbf{e}_n \times \mathbf{e}_n) \text{rot } \mathbf{a}] \tau P_{\pm} = 0. \quad (212)$$

(7) The seventh term can be recast in the form

$$-\frac{\partial \mathbf{a}}{\partial t} \langle \delta \mathbf{b} \otimes \delta \mathbf{v} \rangle^{(1)} = \gamma_A^2 \frac{\partial \mathbf{a}}{\partial t} \left[\sum_{\pm} \int d^3 k \tau \langle \delta \tilde{\mathbf{b}} \otimes \delta \tilde{\mathbf{b}} \rangle_{\pm} \right] \times \text{rot } \mathbf{a}. \quad (213)$$

By comparing the integral in the square brackets with the turbulent magnetic viscosity definition, it is easy to see that it can be written as

$$\sum_{\pm} \int d^3 k \tau \langle \delta \tilde{\mathbf{b}} \otimes \delta \tilde{\mathbf{b}} \rangle_{\pm} = \hat{\mathbf{T}} \frac{\eta_w}{2}. \quad (214)$$

The final expression for the seventh term has the form

$$-\frac{\partial \mathbf{a}}{\partial t} \langle \delta \mathbf{b} \otimes \delta \mathbf{v} \rangle^{(1)} = \left[\left(\hat{\mathbf{T}} \frac{\partial \mathbf{a}}{\partial t} \right) \times \text{rot } \mathbf{a} \right] \frac{\eta_w}{2}. \quad (215)$$

(8) The eighth term contains only the components transverse to the background field:

$$\begin{aligned} \mathbf{a} \left\langle \frac{\partial \delta \mathbf{v}}{\partial t} \otimes \delta \mathbf{b} \right\rangle^{(1)} &= (\gamma_A^2 \mathbf{a} \times \text{rot } \mathbf{a}) \sum_{\pm} \int d^3 k \langle \delta \tilde{\mathbf{b}} \otimes \delta \tilde{\mathbf{b}} \rangle_{\pm} \\ &= (\gamma_A^2 \mathbf{a} \times \text{rot } \mathbf{a}) \frac{W}{2}. \end{aligned} \quad (216)$$

(9) The ninth term contains only anisotropic parts, as well as integrals of the mixed correlators $\langle \delta \tilde{\mathbf{v}} \otimes \delta \tilde{\mathbf{b}} \rangle_{\pm}$; hence, it vanishes:

$$-\mathbf{a} \left\langle \frac{\partial \delta \mathbf{b}}{\partial t} \otimes \delta \mathbf{v} \right\rangle^{(1)} = 0. \quad (217)$$

Collecting all terms together, we obtain the final expression for the force per unit mass:

$$\mathbf{f}_D = \left\{ \left(\frac{\hat{\mathbf{T}}}{2} - \hat{\mathbf{I}} \right) \left[\frac{\partial \mathbf{v}}{\partial t} - \left(\nabla \mathbf{v} + \frac{\eta}{3L_{\parallel}^2} + \frac{\eta}{L_{\perp} \lambda} \right) \mathbf{v} \right] + \frac{1}{2} \gamma_A^2 \mathbf{a} \times \text{rot } \mathbf{a} \right\} \frac{W}{c^2} + \left[\left(\hat{\mathbf{T}} \frac{\partial \mathbf{a}}{\partial t} \right) \times \text{rot } \mathbf{a} \right] \frac{\eta_w}{2c^2}. \quad (218)$$

B. Entropy equation

Here, we present calculations of the turbulent sources for entropy equation (52) related to the displacement current. Terms quadratic in perturbations are

$$\begin{aligned} \frac{q_D}{\eta} = & -\frac{2}{4\pi\rho} \left\langle \frac{1}{c} \frac{\partial \delta^{(1)} \mathbf{E}}{\partial t} \text{rot } \delta \mathbf{B} \right\rangle - \frac{2}{4\pi\rho} \left\langle \frac{1}{c} \frac{\partial \delta^{(2)} \mathbf{E}}{\partial t} \right\rangle \text{rot } \mathbf{B} \\ & + \frac{1}{4\pi\rho} \left\langle \left| \frac{1}{c} \frac{\partial \delta^{(1)} \mathbf{E}}{\partial t} \right|^2 \right\rangle = \frac{1}{c^2} \left(-2\mathbf{a} \left\langle \frac{\partial \delta \mathbf{v}}{\partial t} \times \text{rot } \delta \mathbf{b} \right\rangle \right. \\ & - 2 \text{rot } \mathbf{a} \times \left\langle \frac{\partial \delta \mathbf{v}}{\partial t} \times \delta \mathbf{b} \right\rangle - 2 \text{rot } \mathbf{a} \times \left\langle \delta \mathbf{v} \times \frac{\partial \delta \mathbf{b}}{\partial t} \right\rangle \\ & \left. + \frac{a^2}{c^2} \left\langle \left| \frac{\partial \delta \mathbf{v}}{\partial t} \right|^2 \right\rangle - \left\langle \left(\frac{\mathbf{a}}{c} \frac{\partial \delta \mathbf{v}}{\partial t} \right)^2 \right\rangle \right). \quad (219) \end{aligned}$$

(1) The first term in the right-hand side of (219) arises in the zeroth order of the τ -approximation:

$$\begin{aligned} -2\mathbf{a} \left\langle \frac{\partial \delta \mathbf{v}}{\partial t} \times \text{rot } \delta \mathbf{b} \right\rangle^{(0)} &= -2\mathbf{a} \sum_{\pm} \int d^3k \omega_{\pm} \langle \delta \tilde{\mathbf{v}} \times (\mathbf{k} \times \delta \tilde{\mathbf{b}}) \rangle_{\pm} \\ &= 2\gamma_A^2 a^2 \sum_{\pm} \int d^3k k_{\parallel}^2 P_{\pm} = 2\gamma_A^2 a^2 \frac{W}{3L_{\parallel}^2}. \quad (220) \end{aligned}$$

(2) The second term is nonzero in the first order. It can be processed using (157):

$$\begin{aligned} -2 \text{rot } \mathbf{a} \times \left\langle \frac{\partial \delta \mathbf{v}}{\partial t} \times \delta \mathbf{b} \right\rangle^{(1)} &= -2\gamma_A^2 \text{rot } \mathbf{a} \times \sum_{\pm} \int d^3k \langle (\text{rot } \mathbf{a} \times \delta \tilde{\mathbf{b}}) \times \delta \tilde{\mathbf{b}} \rangle_{\pm} \\ &= [(\hat{\mathbf{T}} \text{rot } \mathbf{a}) \times \text{rot } \mathbf{a}] \gamma_A^2 W. \quad (221) \end{aligned}$$

(3) The third term in the first order contains the vector square of the polarization vector and hence vanishes:

$$\begin{aligned} -2 \text{rot } \mathbf{a} \times \left\langle \delta \mathbf{v} \times \frac{\partial \delta \mathbf{b}}{\partial t} \right\rangle^{(1)} &= 2 \text{rot } \mathbf{a} \sum_{\pm} \int d^3k (\nabla \mathbf{v} + \eta k^2) \langle \delta \tilde{\mathbf{v}} \times \delta \tilde{\mathbf{b}} \rangle_{\pm} = 0. \quad (222) \end{aligned}$$

(4) The fourth term no longer vanishes in the zeroth order:

$$\begin{aligned} \frac{a^2}{c^2} \left\langle \left| \frac{\partial \delta \mathbf{v}}{\partial t} \right|^2 \right\rangle^{(0)} &= \frac{a^2}{c^2} \sum_{\pm} \int d^3k \omega_{\pm}^2 \langle |\delta \tilde{\mathbf{v}}|^2 \rangle_{\pm} \\ &= \left[\gamma_A^2 a^2 + \left(1 - \frac{\gamma_A^2 a^2}{2c^2} \right) v_{\parallel}^2 \right] \frac{\gamma_A^2 a^2}{c^2} \frac{W}{3L_{\parallel}^2} \\ &+ \left(1 - \frac{\gamma_A^2 a^2}{2c^2} \right) \frac{(\gamma_A \mathbf{a} \times \mathbf{v})^2}{c^2} \frac{W}{L_{\perp} \lambda}. \quad (223) \end{aligned}$$

(5) The fifth term arises in the first order of the τ -approximation and can be processed using the triple vector product and expression (157):

$$\begin{aligned} - \left\langle \left(\frac{\mathbf{a}}{c} \frac{\partial \delta \mathbf{v}}{\partial t} \right)^2 \right\rangle^{(1)} &= -\frac{\gamma_A^4}{c^2} \langle [\mathbf{a}, \text{rot } \mathbf{a}, \delta \mathbf{b}]^2 \rangle \\ &= -[\hat{\mathbf{T}} (\gamma_A \mathbf{a} \times \text{rot } \mathbf{a})]^2 \frac{\gamma_A^2 W}{2c^2}. \quad (224) \end{aligned}$$

The final expression for the turbulent heating source has the form

$$\begin{aligned} \frac{q_D}{\eta} = & \frac{(\gamma_A \mathbf{a} \times \mathbf{v})^2}{2c^4} \frac{W}{L_{\perp} \lambda} \\ & + \left\{ 2 + \left[\frac{\gamma_A^2 a^2}{c^2} + \left(1 - \frac{\gamma_A^2 a^2}{2c^2} \right) \frac{v_{\parallel}^2}{c^2} \right] \right\} \frac{a^2}{3L_{\parallel}^2} \frac{\gamma_A^2 W}{c^2} \\ & + [(\hat{\mathbf{T}} \text{rot } \mathbf{a}) \times \text{rot } \mathbf{a}] \frac{\gamma_A^2 W}{c^2} - [\hat{\mathbf{T}} (\gamma_A \mathbf{a} \times \text{rot } \mathbf{a})]^2 \frac{\gamma_A^2 W}{2c^4}. \quad (225) \end{aligned}$$

References

- Landau L D, Lifshitz E M *Electrodynamics of Continuous Media* (New York: Pergamon Press, 1984); Translated from Russian: *Elektrodinamika Sploshnykh Sred* (Moscow: Fizmatlit, 2003)
- Frank-Kamenetskii D A *Lektsii po Fizike Plazmy* (Lecture Notes on Plasma Physics) (Moscow: Atomizdat, 1968)
- Chen F *Introduction to Plasma Physics* (New York: Springer, 1995); Translated into Russian: *Vvedenie v Fiziku Plazmy* (Moscow: Mir, 1987)
- Baranov V B, Krasnobaev K V *Gidrodinamicheskaya Teoriya Kosmicheskoi Plazmy* (Hydrodynamic Theory of Space Plasma) (Moscow: Nauka, 1977)
- Priest E R *Solar Magneto-Hydrodynamics* (Dordrecht: D. Reidel Publ. Co., 1982); Translated into Russian: *Solnechnaya Magnitogidrodinamika* (Moscow: Mir, 1985)
- Lipunov V M *Astrophysics of Neutron Stars* (Heidelberg: Springer, 1992); Translated from Russian: *Astrofizika Neitronnykh Zvezd* (Moscow: Nauka, 1987)
- Priest E R, Hood A W (Eds) *Advances in Solar System Magneto-hydrodynamics* (Cambridge: Cambridge Univ. Press, 1991); Translated into Russian: *Kosmicheskaya Magnitnaya Gidrodinamika* (Moscow: Mir, 1995)
- Campbell C G *Magneto-hydrodynamics in Binary Stars* (Dordrecht: Kluwer Acad. Publ., 1997)
- Beskin V S *MHD Flows in Compact Astrophysical Objects* (Heidelberg: Springer, 2010); Translated from Russian: *Osesimmetrichnye Statsionarnye Techeniya v Astrofizike* (Moscow: Fizmatlit, 2005)
- Warner B *Cataclysmic Variable Stars* (Cambridge: Cambridge Univ. Press, 2003)
- Langer S H, Chanmugam C, Shaviv G *Astrophys. J.* **258** 289 (1982)
- Frank J, King A R, Raine D J *Accretion Power in Astrophysics* 3rd ed. (Cambridge: Cambridge Univ. Press, 2002)
- Bisikalo D V, Zhilkin A G, Boyarchuk A A *Gazodinamika Tesnykh Dvoynykh Zvezd* (Gas Dynamics of Close Binary Systems) (Moscow: Fizmatlit, 2013)
- Galeev A A, in *Fizika Kosmosa. Malen'kaya Entsiklopediya* (Physics of Cosmos. Small Encyclopedia) (Ed. R A Sunyaev) 2nd ed. (Moscow: Sovetskaya Entsiklopediya, 1986) p. 367
- Potter D *Computational Physics* (London: J. Wiley 1973); Translated into Russian: *Vychislitel'nye Metody v Fizike* (Moscow: Mir, 1975)
- Kulikovskii A G, Pogorelov N V, Semenov A Yu *Mathematical Aspects of Numerical Solution of Hyperbolic Systems* (Boca Raton, Fla.: Chapman and Hall. CRC, 2000); Translated from Russian: *Matematicheskie Voprosy Chislenogo Resheniya Giperbolicheskikh Sistem Uravnenii* (Moscow: Fizmatlit, 2001)

17. Boris J P “A physically motivated solution of the Alfvén problem”, NRL Memorandum Report 2167 (Washington, DC: Naval Research Laboratory, 1970)
18. Gombosi T I et al. *J. Comput. Phys.* **177** 176 (2002)
19. Tóth G et al. *J. Geophys. Res.* **116** A07211 (2011)
20. Zakharov V E *J. Appl. Mech. Tech. Phys.* **6** 10 (1965); *Zh. Prikl. Mekh. Tekh. Fiz.* (1) 14 (1965)
21. Zakharov V E *J. Appl. Mech. Tech. Phys.* **6** 22 (1965); *Zh. Prikl. Mekh. Tekh. Fiz.* (4) 35 (1965)
22. Iroshnikov P S *Sov. Astron.* **7** 566 (1964); *Astron. Zh.* **40** 742 (1963)
23. Kraichnan R H *Phys. Fluids* **85** 575 (1965)
24. Galtier S et al. *J. Plasma Phys.* **63** 447 (2000)
25. Kuznetsov E A *JETP* **93** 1052 (2001); *Zh. Eksp. Teor. Fiz.* **120** 1213 (2001)
26. Chandran B D G *Phys. Rev. Lett.* **95** 265004 (2005)
27. Zhilkin A G, Bisikalo D V *Astron. Rep.* **54** 840 (2010); *Astron. Zh.* **87** 913 (2010)
28. Zhilkin A G, Bisikalo D V, Boyarchuk A A *Phys. Usp.* **55** 115 (2012); *Usp. Fiz. Nauk* **182** 121 (2012)
29. Zhilkin A G, Bisikalo D V, Ustyugov V A *AIP Conf. Proc.* **1551** 22 (2013)
30. Zhilkin A G, Bisikalo D V, Mason P A *Astron. Rep.* **56** 257 (2012); *Astron. Zh.* **89** 291 (2012)
31. Bisikalo D V et al. *Astron. Rep.* **57** 327 (2013); *Astron. Zh.* **90** 366 (2013)
32. Fateeva A M, Zhilkin A G, Bisikalo D V *Astron. Rep.* **60** 87 (2015); *Astron. Zh.* **92** 977 (2015)
33. Isakova P B, Zhilkin A G, Bisikalo D V *Astron. Rep.* **59** 843 (2015); *Astron. Zh.* **92** 720 (2015)
34. Isakova P B et al. *Astron. Rep.* **60** 498 (2016); *Astron. Zh.* **93** 474 (2016); Isakova P B et al. *Astron. Rep.* **61** 560 (2017); *Astron. Zh.* **94** 566 (2017)
35. Sridhar S, Goldreich P *Astrophys. J.* **432** 612 (1994)
36. Goldreich P, Sridhar S *Astrophys. J.* **438** 763 (1995)
37. Bruno R, Carbone V *Living Rev. Solar Phys.* **10** 2 (2013)
38. Canuto V M *Astrophys. J.* **482** 827 (1997)
39. Chernyshov A A, Karelsky K V, Petrosyan A S *Phys. Usp.* **57** 421 (2014); *Usp. Fiz. Nauk* **184** 457 (2014)
40. Landau L D, Lifshitz E M *Fluid Mechanics* (Oxford: Pergamon Press, 1987); Translated from Russian: *Gidrodinamika* (Moscow: Fizmatlit, 2003)
41. Okamoto I *Astron. Astrophys.* **211** 476 (1989)
42. Gershman B N, Erukhimov L M, Yashin Yu Ya *Volnovye Yavleniya v Ionosfere i Kosmicheskoi Plazme* (Wave Phenomena in Ionosphere and Space Plasma) (Moscow: Nauka, 1984)
43. Braginskii S I *Sov. Phys. JETP* **10** 1005 (1960); *Zh. Eksp. Teor. Fiz.* **37** 1417 (1959)